(12) INTERNATIONAL APPLICATION PUBLISHED UNDER THE PATENT COOPERATION TREATY (PCT)

(19) World Intellectual Property Organization
International Bureau

(43) International Publication Date
26 October 2012 (26.10.2012)

WIPO | PCT

(10) International Publication Number
WO 2012/143798 A1

(51) International Patent Classification:
*A61B 6/14* (2006.01) *A61C 8/00* (2006.01)

(21) International Application Number:
PCT/IB2012/050045

(22) International Filing Date:
4 January 2012 (04.01.2012)

(25) Filing Language: English

(26) Publication Language: English

(30) Priority Data:
61/477,787 21 April 2011 (21.04.2011) US
13/329,557 19 December 2011 (19.12.2011) US

(71) Applicant *(for all designated States except US)*: **DR. HASSAN GHADERI MOGHADDAM** [CA/CA]; 3409 Carling ave., Ottawa, Ontario K2H 7V5 (CA).

(72) Inventors; and

(75) Inventors/Applicants *(for US only)*: **MOGHADDAM, Hassan, Ghaderi** [CA/CA]; 3409 Carling ave., Ottawa, Ontario K2H 7V5 (CA). **GALLANT, Pascal** [CA/CA]; 1406 Auclair Blvd., Québec, Québec G2G 2H2 (CA). **MERMUT, Ozzy** [CA/CA]; 1206 Des Cornalines St, Québec, Québec G2L 3H1 (CA). **VEILLEUX, Israël** [CA/CA]; 167 Rang C, Sainte-Rose-de-Watford, Québec G0R 4G0 (CA).

(74) Agent: **FASKEN MARTINEAU DUMOULIN LLP**; Suite 800, 140 Grande Allée East, Québec, Québec G1R 5M8 (CA).

(81) Designated States *(unless otherwise indicated, for every kind of national protection available)*: AE, AG, AL, AM, AO, AT, AU, AZ, BA, BB, BG, BH, BR, BW, BY, BZ, CA, CH, CL, CN, CO, CR, CU, CZ, DE, DK, DM, DO, DZ, EC, EE, EG, ES, FI, GB, GD, GE, GH, GM, GT, HN, HR, HU, ID, IL, IN, IS, JP, KE, KG, KM, KN, KP, KR, KZ, LA, LC, LK, LR, LS, LT, LU, LY, MA, MD, ME, MG, MK, MN, MW, MX, MY, MZ, NA, NG, NI, NO, NZ, OM, PE, PG, PH, PL, PT, QA, RO, RS, RU, RW, SC, SD, SE, SG, SK, SL, SM, ST, SV, SY, TH, TJ, TM, TN, TR, TT, TZ, UA, UG, US, UZ, VC, VN, ZA, ZM, ZW.

(84) Designated States *(unless otherwise indicated, for every kind of regional protection available)*: ARIPO (BW, GH, GM, KE, LR, LS, MW, MZ, NA, RW, SD, SL, SZ, TZ, UG, ZM, ZW), Eurasian (AM, AZ, BY, KG, KZ, MD, RU, TJ, TM), European (AL, AT, BE, BG, CH, CY, CZ, DE, DK, EE, ES, FI, FR, GB, GR, HR, HU, IE, IS, IT, LT, LU, LV, MC, MK, MT, NL, NO, PL, PT, RO, RS, SE, SI, SK, SM, TR), OAPI (BF, BJ, CF, CG, CI, CM, GA, GN, GQ, GW, ML, MR, NE, SN, TD, TG).

**Published**:

— *with international search report (Art. 21(3))*

(54) **Title**: METHOD AND SYSTEM FOR OPTICALLY EVALUATING PROXIMITY TO THE INFERIOR ALVEOLAR NERVE IN SITU

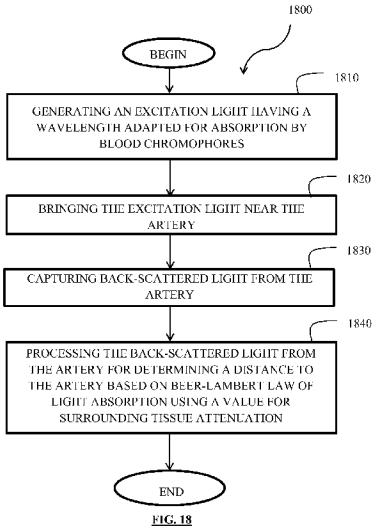

FIG. 18

(57) **Abstract**: A low coherence interferometry probe system for evaluating proximity to a tissue layer, comprising a low coherence light source for generating low coherence excitation light, an excitation optical fiber to bring the low coherence excitation light near the tissue layer and a collection optical fiber for capturing back-scattered light from the tissue layer. The probe system comprises a low coherence interferometry sub-system and a digital signal processor for evaluating a distance to the tissue layer based on the back- scattered light received by the collection optical fiber. There is also provided a spectral absorption probe system for evaluating proximity to an artery, comprising a light source for generating excitation light having a wavelength adapted for absorption by blood chromophores, an excitation optical fiber to bring the excitation light near the artery and a collection optical fiber for capturing back-scattered light from the artery. The probe system comprises a light detector and a signal processor for determining a distance to the artery based on the back-scattered light and on Beer-Lambert law of light absorption using a value for surrounding tissue attenuation coefficient (μείί). A spectral absorption and low coherence interferometry probe system combining low coherence interferometry and spectral absorption is also provided.

WO 2012/143798 A1

# METHOD AND SYSTEM FOR OPTICALLY EVALUATING PROXIMITY TO THE INFERIOR ALVEOLAR NERVE IN SITU

## CROSS_REFERENCE TO RELATED APPLICATION

**[0001]** This application claims priority of US Provisional Patent Application serial number 61/477,787 filed on April 21, 2011 and entitled "METHOD AND SYSTEM FOR OPTICALLY EVALUATING PROXIMITY TO THE INFERIOR ALVEOLAR NERVE IN SITU" and of US Patent Application serial number 13/329,557 filed on December 19, 2011 and entitled "METHOD AND SYSTEM FOR OPTICALLY EVALUATING PROXIMITY TO THE INFERIOR ALVEOLAR NERVE IN SITU", the specifications of which are hereby incorporated by reference.

## TECHNICAL FIELD

**[0002]** The invention relates to methods and systems for evaluating proximity to a target, more specifically, for evaluating proximity to a nerve.

## BACKGROUND OF THE ART

**[0003]** Dental implants are a widely accepted treatment for the partially or completely edentulous patient. Dental implants are the fastest growing procedure in dentistry today. It is a 1 billion dollar industry in the USA. Dental implants offer a suitable alternative to mucosal adhering dentures and allow a more natural option for the patient. Implants have a high success rate when given proper care and when post-surgical instructions are followed. Dental implants can be in the form of a single tooth replacement, or can replace a series or an entire set of teeth. The basic implant procedure involves drilling a channel in the mandible where an artificial root is surgically inserted. A dental prosthesis is then placed onto the frame of the artificial root. Within a few months of recovery, the patient should have a fully integrated and functional prosthesis.

**[0004]** Implant procedures are not without complications. The goal of an implant procedure is to attain a successful level of osseointegration. Osseointegration is defined as the

direct anchorage of an implant by the formation of bony tissue around the implant without the growth of fibrous tissue at the bone-implant interface. Implants surrounded with fibrous tissue show mobility when a load is applied. The successfully osseointegrated implant shows no mobility when loaded. Other major factors for the successful implant depend mainly on the type of jaw treated, the density of the bone, and the length of the implant. Implant length is the depth created by the surgeon upon drilling a channel in the mandible. Short implants have a length of less than 10 mm and are noted to have larger failure rates. Hence the need to create sufficient length for successful osseointegration of implants within the mandible is a priority.

**[0005]** However, the drilling of a large implant channel within the mandible carries a risk of breaching an intraosseous canal which encloses the inferior alveolar nerve (IAN). Disruption of the IAN can lead to loss of sensation in the anterior mandible area, such as paresthesia or numbness to the lower lip, due to the disruption of the mental nerve, which is the terminal branch of the IAN and is the neural bundle serving this area. The loss of sensation for the patient is certainly undesirable.

**[0006]** The reported incidence of nerve injury from implant placement in the literature is highly variable and ranges depending on the study from 0% to as high as 44% (Misch and Resnik Implant Dentistry 2010; 19:378-386). A survey at the Misch international institute indicated that 73% of dentists have encountered neurosensory impairment within their practice. To help prevent nerve injury, patients can be subjected to CT scans which are costly and also involve radiation. The standard error for a CT scan is still in the range of 1.7 mm. This measurement error can result in nerve damage.

**[0007]** There is thus a need to develop a surgical drill which is able to detect the proximity and/or location of the IAN in the mandible, preferably during implant procedures. The sensor device should allow the drill to approach closely, but not impair or damage the IAN within an acceptable error limit of the intraosseous canal. Hence, a system that automatically terminates drill action when in close range of the IAN would be most desirable.

## SUMMARY

**[0008]** According to one broad aspect of the present invention, there is provided a spectral absorption probe system for evaluating proximity to an artery, comprising a light source for generating excitation light having a wavelength adapted for absorption by blood chromophores, an excitation optical fiber to bring the excitation light near the artery and a collection optical fiber for capturing back-scattered light from the artery. The spectral absorption probe system comprises a light detector operatively connected to the collection optical fiber and a signal processor operatively connected to the light detector for determining a distance to the artery based on the back-scattered light and on Beer-Lambert law of light absorption using a value for surrounding tissue attenuation coefficient (μeff).

**[0009]** In one embodiment, the spectral absorption probe system further comprises a biocompatible metallic rod surrounding the excitation optical fiber and the collection optical fiber.

**[0010]** In one embodiment, the excitation optical fiber and the collection optical fiber are provided in a single double-clad optical fiber with a fiber core of the double-clad optical fiber bringing the excitation light near the artery and a first clad of the double-clad optical fiber capturing the back-scattered light from the artery.

**[0011]** In one embodiment, the probe system is fibered and integrated within a hollow core of a drill bit.

**[0012]** In one embodiment, an operating depth range of the probe system is comprised between 1 mm and 5 mm.

**[0013]** In one embodiment, the light source is selected from a group consisting of a LED, a laser and a set of light source units.

**[0014]** In a further embodiment, the wavelength of the light source is comprised between 650 nm and 900 nm.

**[0015]** In one embodiment, the spectral absorption probe system further comprises an additional light source having a wavelength adapted for absorption by blood chromophores,

the wavelengths of the light source and of the additional light source being each comprised between 650 nm and 900 nm.

**[0016]** In one embodiment, the light detector is selected from a group consisting of a photodiode, an avalanche photodiode (APD), a photomultiplier tube (PMT) and a camera.

**[0017]** In one embodiment, the spectral absorption probe system further comprises a calibration unit having a pulse oxymeter for monitoring oxygen saturation levels to maintain an inline calibration of arterial blood absorption properties.

**[0018]** In one embodiment, the surrounding tissue attenuation coefficient (μeff) is determined according to absorption and scattering in surrounding tissue of a calibration excitation signal.

**[0019]** In one embodiment, the signal processor comprises a lock-in amplifier and a heterodyning processing circuit connected thereto.

**[0020]** In one embodiment, the light detector is AC-coupled to the signal processor.

**[0021]** In another embodiment, the excitation optical fiber and the collection optical fiber are separated from each other and extend angularly.

**[0022]** In a further embodiment, a single one of the excitation optical fiber and the collection optical fiber is integrated within a hollow core of a drill bit.

**[0023]** According to another broad aspect of the present invention, there is provided a low coherence interferometry probe system for evaluating proximity to a tissue layer, comprising a low coherence light source for generating low coherence excitation light, an excitation optical fiber to bring the low coherence excitation light near the tissue layer and a collection optical fiber for capturing back-scattered light from the tissue layer. The low coherence interferometry probe system comprises a low coherence interferometry sub-system operatively connected to the excitation optical fiber and the collection optical fiber and having a beam splitter and a reference mirror. The low coherence interferometry probe system comprises a digital signal processor operatively connected to the low coherence interferometry sub-system

for evaluating a distance to the tissue layer based on the back-scattered light received by the collection optical fiber.

**[0024]** In one embodiment, the tissue layer is selected from a group consisting of a canal wall, an artery, a nerve, a neurovascular bundle and a sinus floor.

**[0025]** In one embodiment, the probe system is fibered and integrated within a hollow core of a drill bit.

**[0026]** In one embodiment, the low coherence light source is selected from a group consisting of a superluminescent LED, a pulsed laser and a frequency-swept laser source.

**[0027]** In one embodiment, an operating depth range of the probe system is comprised between 1 mm and 5 mm.

**[0028]** In one embodiment, the excitation optical fiber and the collection optical fiber are both embedded in a single-mode optical fiber.

**[0029]** In another embodiment, the excitation optical fiber and the collection optical fiber are provided in a single double-clad optical fiber having a core acting as an excitation channel, an inner clad acting as a collection channel and an outer clad surrounding the inner cladding.

**[0030]** In one embodiment, the probe system is operated in A-mode.

**[0031]** In another embodiment, the probe system comprises a forward-looking transverse scanner enabling B-mode imaging.

**[0032]** In a further embodiment, the excitation optical fiber and the collection optical fiber are both embedded in a rotating beveled double-clad optical fiber having a core acting as an excitation channel, an inner cladding acting as a collection channel and an outer cladding surrounding the inner cladding, the probe system being operated in a B-mode providing conical imaging.

**[0033]** In one embodiment, the probe system further comprises at least one of a Doppler OCT unit for performing Doppler measurements and a speckle variance OCT unit.

**[0034]** According to another broad aspect of the present invention, there is provided a spectral absorption and low coherence interferometry probe system for evaluating proximity to a tissue layer, comprising a light source for generating excitation light having at least one wavelength adapted for absorption by blood chromophores and low coherence, an excitation optical fiber to bring the excitation light near the tissue layer and a collection optical fiber for capturing back-scattered light from the tissue layer. The probe system comprises a light detector operatively connected to the collection optical fiber and a digital signal processor operatively connected to the light detector for determining a distance to the tissue layer based on the back-scattered light and on Beer-Lambert law of light absorption using a value for surrounding tissue attenuation coefficient (μeff). The probe system comprises a low coherence interferometry sub-system operatively connected to the excitation optical fiber and the collection optical fiber and having a beam splitter and a reference mirror. The probe system also comprises a signal processor operatively connected to the low coherence interferometry sub-system for evaluating a distance to the tissue layer based on the back-scattered light received by the collection optical fiber.

**[0035]** In one embodiment, the excitation optical fiber comprises a single mode fiber and the collection optical fiber comprises a single mode fiber for OCT mode light collection and a multimode fiber for spectral absorption mode light collection.

**[0036]** In a further embodiment, the probe system comprises a forward-looking transverse scanner enabling B-mode imaging.

**[0037]** According to another broad aspect of the present invention, there is provided a spectral absorption probe method for evaluating proximity to an artery, comprising: generating an excitation light having a wavelength adapted for absorption by blood chromophores; bringing the excitation light near the artery; capturing back-scattered light from the artery; and processing the back-scattered light from the artery for determining a distance to the artery based on Beer-Lambert law of light absorption using a value for surrounding tissue attenuation coefficient (μeff).

**[0038]** In one embodiment, the method is used for evaluating proximity to an inferior alveolar nerve in situ.

**[0039]** In one embodiment, the method further comprises monitoring oxygen saturation levels to maintain an inline calibration of arterial blood absorption properties.

**[0040]** In one embodiment, the method further comprises determining the surrounding tissue attenuation coefficient (μeff) according to absorption and scattering in surrounding tissue of a calibration excitation signal.

**[0041]** In one embodiment, the back-scattered light is captured angularly and at a given distance with respect to the brought excitation light.

**[0042]** In one embodiment, the method further comprises using a vascular contrast agent.

**[0043]** According to another broad aspect of the present invention, there is provided a low coherence interferometry probe method for evaluating proximity to a tissue layer, comprising: generating a low coherence excitation light; bringing the low coherence excitation light near the tissue layer; capturing back-scattered light from the tissue layer; performing interferometry between the low coherence excitation light and the back-scattered light for providing an interference signal; and processing the interference signal for evaluating a distance to the tissue layer.

**[0044]** In one embodiment, the method is used for evaluating proximity to an inferior alveolar nerve in situ.

**[0045]** In one embodiment, the probe method is operated according to A-mode.

**[0046]** In another embodiment, the method further comprises forward-looking transverse scanning of the tissue layer for enabling B-mode imaging.

**[0047]** In one embodiment, the method further comprises using an optical clearing agent at a probing site.

**[0048]** According to another broad aspect of the present invention, there is provided a spectral absorption and low coherence interferometry probe method for evaluating proximity to a tissue layer, comprising: generating an excitation light having at least one wavelength adapted for absorption by blood chromophores and low coherence; bringing the excitation

light near the tissue layer; capturing back-scattered light from the tissue layer; processing the back-scattered light for determining a first distance to the tissue layer based on Beer-Lambert law of light absorption using a value for surrounding tissue attenuation coefficient (μeff); performing interferometry between the low coherence excitation light and the back-scattered light for providing an interference signal; and processing the interference signal for evaluating a second distance to the tissue layer.

## BRIEF DESCRIPTION OF THE DRAWINGS

**[0049]** Having thus generally described the nature of the invention, reference will now be made to the accompanying drawings, showing by way of illustration a preferred embodiment thereof and in which:

**[0050]** FIG. 1 is a sagittal section of a mandible showing the inferior alveolar nerve (IAN) positioned directly underneath the molar teeth;

**[0051]** FIG. 2 is a sagittal section of the inferior alveolar nerve (IAN) positioned at the bottom of the mandible;

**[0052]** FIG. 3 (Prior Art) is a diagram of a standard time-domain Optical Coherence Tomography setup of the prior art;

**[0053]** FIG. 4A (Prior Art) is a diagram of a spatially-encoded Fourier-domain OCT system (SEFD-OCT);

**[0054]** FIG. 4B (Prior Art) is a diagram of a frequency-swept-source-based OCT system, or time-encoded Fourier-Domain OCT system (TEFD-OCT);

**[0055]** FIG. 5 is a schematics of a low coherence interferometry probe system for evaluating proximity to a tissue layer, according to one embodiment.

**[0056]** FIG. 6 is a concept schematics of a drill-integrated IAN sensor based on the NIR spectral absorption technique, according to one embodiment;

**[0057]** FIG. 7 is a schematics of a spectral absorption probe system for evaluating proximity to an artery, according to one embodiment.

**[0058]** FIG. 8 is a graph illustrating impact of propagation in a turbid medium such as biological tissue on an intensity-modulated light beam;

**[0059]** FIG. 9 is a schematics of a heterodyne detection configuration for a IAN sensor, according to one embodiment;

**[0060]** FIG. 10A is a schematics of an embodiment of a standalone IAN proximity sensor handpiece, according to a spectral absorption configuration;

**[0061]** FIG. 10B is a schematics of another embodiment of a standalone IAN proximity sensor handpiece, according to a OCT-based, single fiber configuration;

**[0062]** FIG. 11 is a schematics showing a disjointed spectral absorption IAN sensor configuration, according to one embodiment;

**[0063]** FIG. 12 is a diagram of a double-clad optical fiber-based IAN sensor handpiece design, according to one embodiment;

**[0064]** FIG. 13 is a diagram of a spectral absorption-based IAN sensor apparatus where a pulse oxymeter is used, according to one embodiment;

**[0065]** FIG. 14 is a schematics of another IAN sensor using a conical scanning principle, according to another embodiment;

**[0066]** FIG. 15A is a diagram of a drill-integrated IAN sensor using an optical fiber rotary joint, according to one embodiment;

**[0067]** FIG. 15B is a diagram of a drill-integrated IAN sensor using a non-contact optical coupling, according to another embodiment;

**[0068]** FIG. 16 is a diagram of a one dimensional model of a trabecular bone, according to one embodiment.

**[0069]** FIG. 17 is a flow chart of a probe method for evaluating proximity to a tissue layer, according to one embodiment.

**[0070]** FIG. 18 is a flow chart of a probe method for evaluating proximity to an artery, according to one embodiment.

**[0071]** It will be noted that throughout the appended drawings, like features are identified by like reference numerals.

## DETAILED DESCRIPTION

**[0072]** **Anatomy background**

**[0073]** Referring to FIGS. 1 and 2 which show Sagittal sections of a mandible **10**, the inferior alveolar nerve **12** (IAN) is a branch of the mandibular nerve, which stems from the trigeminal nerve system. The IAN **12** enters an intraosseous canal through the mandibular foramen in the posterior portion of the mandible. The nerve continues its path within the mandible **10** and then exits through the mental foramen. Throughout the length of the osseous canal, the IAN **12** is closely associated with the inferior alveolar artery and both structures are covered in a tough sheath of connective tissue. The diameter of the entire bundle varies between patients but averages at 2.53±0.29 mm [*C.D. Morris et al., J. Oral Maxillo. Surg., 68:2833-2836, 2010*].

**[0074]** The intraosseous canal is a hollow channel and in most cases has borders with defined walls which may be consistent throughout the length of the canal. The diameter of this canal is known to be 2.0 to 2.6 mm. The canal walls may either be composed of cortical bone, or in lesser frequency, may be continuous and uniform with the surrounding trabecular bone. Many patients have canals which abruptly become uniform and continuous with surrounding cancellous bone within proximity of the mental foramen. Although the intraosseous canal is present in many patients, it is not a consistent feature within the mandibles of every individual. Dissection studies show that cortical walls and distinct osseous canals within mandibles are not always present. Some specimens of IAN were shown to travel the trabecular marrow spaces without any defined canal present.

**[0075]** The position of the IAN **12** within the mandible **10** is highly variable. In one dissection study, the position of the IAN varied in position from the sub-dental portion below the molar roots (See FIG. 1), to an inferior position near the bottom ridge of the mandible **10** (See FIG. 2). A feature which was not frequent, but was observed, was the splitting of the IAN bundle into diffuse branches without a defined intraosseous canal.

**[0076]** **Current IAN Location Methods**

**[0077]** The general imaging methods currently used by surgeons to assess the position of the IAN are Panoramic X-ray, Computed Tomography (CT) scan, and Microradiograph (MR) imaging. As some patients may lack an osseous canal and an IAN bundle altogether, pre-operative imaging is imperative. X-rays are usually taken in a panoramic fashion, encircling the entire mandible. This presents a global view of the mandible and images potential implant placement sites. The limitations of this technique are that it provides no information about mandible thickness and suffers from a distortion factor of about 25%. A more modern approach to the imaging of the mandible is the CT scan. This method is able to generate over-lapping images through computer software programs. However, for dental surgical purposes, only bone and calcified structures are imaged by CT; the IAN and associated non-osseous tissues are not. Thus the CT scan is limited for patients without defined canal walls; locating the IAN on a single cross section is difficult. Reformatted images of adjacent parallel and perpendicular images must be taken and used to assess the exact relative location of the IAN within the mandible. Detailed X-ray imaging, or Mircoradiograph (MR) imaging, is able to image and provide a notable contrast between osseous and non-osseous tissues. When using MR, the canal is visible in cross-sectional reformations exclusive of the osseous tissue surrounding it. The drawback to using MR imaging is that spatial distortions on MR images may not give proper resolution for smaller distances. This is also true for both CT and Panoramic scans, although the resolution for both these techniques has been shown to be similar. Current CT based technologies are expanding imaging possibilities by integrating novel software and 3-D imaging methods.

**[0078]** The drawback for all these imaging methods, with the exception of novel 3-D CT scanning methods, is that they are not in real time and must be performed preoperatively

before the surgical procedure. These methods are also limited in resolution (typ. ±1.3mm) and may not be able to properly image diffuse IAN layouts for patients without a localized IAN bundle. This adds much uncertainty and leaves the surgeon to estimate the exact locations of the IAN during surgery. Thus, a technology which combines both the procedures of drilling and localization of the IAN into a simultaneous process has yet to be developed.

**[0079] Machining of Bone and Present Drill Sensor Technology**

**[0080]** In the process of dental implants, drilling is used to create channels within the mandible for the placement of artificial roots.

**[0081]** The drilling operation performed on the mandible must traverse a cortical bone layer and into a cancellous bone mass. As the drill continues forward, heat is generated at the apex of the drill bit. Some of this heat is absorbed by the surrounding bone, raising its temperature. An implication of temperature rise and heat generation from machining bone is thermal osteonecrosis. Irreversible thermal osteonecrosis occurs when bone temperature reaches and exceeds 47°C. With irreversible osteonecrosis, adequate osseointegration could be inhibited, thus reducing the chances for a successful implant. When drilling bone without external irrigation, tissue temperatures can range from 31-56°C. An irrigation system is included in most surgical drills for this purpose. Water is injected through an orifice from the apex of the drill bit into the immediate drilling site. This acts to cool the drilling site, and functions to prevent thermal osteonecrosis. For the contribution of heat generation from the drill itself, the most important parameters are drill speed, feed rate and drill diameter. Hence with irrigation, adjustment and control of these parameters can help to reduce heat generation when drilling in bone.

**[0082]** Currently, drill sensor technology is not aimed at discerning the media situated at the drill-bone interface. Technology is more focused on detecting and imaging wear on drill burs and machinery. There exists drill detection systems aimed at bone machining applications. A mechatronic system developed by Bouazza-Marouf and Ong [Ong, F.R., Bouazza-Marouf, K.; 1999; The detection of drill bit break-through for the enhancement of safety in mechatronic assisted orthopaedic drilling; MECHATRONICS 9: 565-588] is able to discern drill break-through from inherent fluctuations in bone structure when drilling long

bones. This system is able to detect differences in force through an electronic logic algorithm. The drawback here is that a certain, constant force is applied and the drill bit feed rate into the bone media is constant. In practice, drilling with constant force and feed rate would not be used due to variability in bony tissues within the body and between patients. The mechatronic system was also not able to discern latent non-osseous tissue. The application of this system for the purpose of long implant placement within the mandible would not be desirable as bone breakthrough is the arresting factor for this system.

**[0083] Optical-based *in situ* proximity IAN sensor**

**[0084]** Current surgery practice allows for an experienced dental surgeon to drill the mandible down to a distance of 2 mm from the IAN, without too much risk of damaging the nerve bundle. As such, the proximity sensor operating range should be within this 2 mm boundary, although a longer distance of operation would be useful. At the same time, the axial resolution of the sensor should be as high as possible.

**[0085]** The first approach is based on Low Coherence Interferometry (LCI). A LCI probe can be built to operate in A-mode (i.e. point-scan only, no image). LCI presents similar results to ultrasound echolocation and provides a high-resolution measurement of the tissue layers structure based on back-scattered light intensity from those layers. The measurements being optical in nature, the axial resolution of this technique is at least ten times better than with ultrasound, at the cost of a much lower depth penetration (typ. resolutions in ~10 µm at maximal depths of ~1.5 mm, depending on tissues optical absorption and scattering properties). The particular imaging extension of this technique, i.e B-mode scanning, is known in the art as Optical Coherence Tomography (OCT).

**[0086]** FIG. 3 shows an embodiment of a standard time-domain LCI or OCT system **30** using a low coherence light source **32** (typically a superluminescent LED or pulsed laser) and an interferometer configuration **34** for performing a longitudinal scanning **36** and a lateral scanning **38**. As illustrated, an optical arrangement **40** is used for implementing the lateral scanning **38** while an optical arrangement **42** comprising a moving mirror **44** is used for implementing the longitudinal scanning **36**. A signal processor **46** may be used in conjunction with a computer **48** for signal processing purposes. Newer designs, as the systems **50** and **52**

shown in FIGS. 4A and 4B respectively, involve detecting in the Fourier domain or using frequency-swept light sources to disband with the traditional time-pulsed requirement of the incident light emission. The system **50** comprises a low coherence source (LCS) **54**, an interferometer sub-assembly **56** provided with a beamsplitter (BS) **58** and a reference mirror (REF) **60**. The system **50** also comprises a diffraction grating (DG) **62** and a camera (CAM) **64** for detecting light back-scattered by the sample (SMP) **66**. A digital signal processor (DSP) **68** is operatively connected to the camera **64** for providing an OCT image based on the back-scattered light. The system **52** of FIG. 4B uses a swept source (SS) **72** in place of the low coherence source **54** of FIG. 4A and a photodetector (PD) **70**.

**[0087]** An A-Mode fibered LCI probe can be designed in a compact form small enough to fit within a dental drill bit, according to one embodiment. Tissue interfaces will appear as an increase in the back-scattered signal intensity. Similarly, in an alternative embodiment, a B-mode 2D image can be generated by building the LCI / OCT probe with an integrated forward-looking proximal or distal scanner, as it should become apparent to the skilled addressee. In the case of the IAN, an interface signal will be generated either by the canal wall or the nerve bundle itself and will be visible in real time to the dental surgeon as long as the interface is within the penetration depth range of the instrument.

**[0088]** FIG. 5 illustrates a low coherence interferometry probe system **100** for evaluating proximity to a tissue layer **102**, according to the above detailed technique and according to one embodiment. The probe system **100** comprises a low coherence light source **104** for generating low coherence excitation light **106**, an excitation optical fiber **108** to bring the low coherence excitation light **106** near the tissue layer **102** and a collection optical fiber **110** for capturing back-scattered light from the tissue layer **102**. The probe system **100** also comprises a low coherence interferometry sub-system **112** operatively connected to the excitation optical fiber **108** and the collection optical fiber **110** and having a beam splitter **114** and a reference mirror **116**. A digital signal processor **118** operatively connected to the low coherence interferometry sub-system **112** is used for evaluating a distance **120** to the tissue layer **102** based on the back-scattered light received by the collection optical fiber **110**.

**[0089]** FIG. 17 illustrates a low coherence interferometry probe method for evaluating proximity to a tissue layer, according to one embodiment. According to processing step **1710**, a low coherence excitation light is generated. According to processing step **1720**, the low coherence excitation light is brought near the tissue layer. According to step **1730**, back-scattered light from the tissue layer is captured. According to processing step **1740**, interferometry between the low coherence excitation light and the back-scattered light is performed for providing an interference signal. According to processing step **1750**, the interference signal is processed for evaluating a distance to the tissue layer.

**[0090]** Experiments were conducted with a probe system **100** on a post-mortem extracted human jawbone cut in such a way that the LCI entry point surface made a wedge with the approximate location of the canal, thus providing increased depth of the IAN interface with the entry point location. This approach allows to evaluate the depth penetration of the technique. The results indicate a probing range of about 1 mm within the test conditions (ex vivo sample, wavelength of 1.32 µm). An increase in wavelength should improve detection range as tissue scattering decrease monotonically with wavelength. However, one must also fine tune the wavelength so that it fits between tissue absorption lines that are numerous in these ranges due to tissue water content. Appropriate designs for performing LCI / OCT systems seem to favor the use of frequency-swept laser sources for state-of-the-art devices. Availability of such light sources at 1.55 µm is increasing and development at 1.8 µm is ongoing. The skilled addressee will nevertheless appreciate that other arrangements may be considered.

**[0091]** A second optical approach is to use the spectral absorption properties of arterial blood and the blood flow dynamics (change in blood volume due to the patient's pulse) to measure the distance to this artery based on the Beer-Lambert law of light absorption:

**[0092]** $$I = I_0 \exp(-\mu_{eff} d) \quad [1]$$

**[0093]** where $I$ and $I_0$ are the detected and incident light intensities, respectively, $d$ is the total propagation distance of the light within tissues ( the sensor will measure the distance $s = d/2$ ) and $\mu_{eff}$ is the attenuation coefficient of the medium in which light propagation

occurs. In the case of tissues, attenuation is a combination of absorption and scattering of the photons at the illumination wavelength and is tissue-type-dependent.

**[0094]** A first approximation model can provide an evaluation of the order of magnitude of the return signal. The probing device would operate from within the trabecular bone to identify the artery from the IAN neurovascular bundle. Trabecular bone is a complex structure composed of cortical bone and bone marrow arranged in "cells", similar to a beehive. Optically, this structure may be represented in a one dimensional model **200** where three layers **202**, **204**, **206** are stacked vertically, each representing cortical bone, bone marrow and arterial blood, as illustrated in FIG. 16. In this model, the blood layer thickness varies over time in a periodic fashion to represent the blood volume change in the arteries due to the cardiac cycle. The thickness of the bone and marrow layers is dependent on the porosity of the trabecular structure.

**[0095]** Using this representation, the equations governing the optical propagation, based on the Beer-Lambert's Law, are:

**[0096]**
$$I = I_0 e^{-[\mu_{marrow} d_{marrow} + \mu_{cortical} d_{cortical} + \mu_{HbO2}(t) d_{HbO2}(t)]} \quad (2),$$

**[0097]** where $\mu_x$ and $d_x$ (x = *marrow, cortical, HbO2*) are the attenuation coefficient and layer thickness of each of the three types of tissue involved. The marrow and cortical layer thicknesses are related to the porosity of the trabecular structure $0 < p < 1$ such that:

**[0098]** $d_{marrow} = p \times d_{total}$

**[0099]** $d_{cortical} = (1-p) \times d_{total}$ (3),

**[00100]** where $d_{total} = d_{marrow} + d_{cortical}$ is the total thickness of trabecular bone between the light input and the arterial layer. Because of blood flow and its properties, the HbO2 terms are time-dependent. Indeed, the distance parameter $d_{HbO2}$ will change due to the volume variation

occurring with pulsating blood flow. In the proposed model **200**, this is represented by a harmonic variation of the thickness of the arterial layer:

**[00101]** $$d_{HbO2}(t) = d_{HbO2-baseline}(1 + \Delta_d \cos(2\pi f t)) \quad (4),$$

**[00102]** where $d_{HbO2\text{-}baseline}$ is the average thickness of the layer, $0 < \Delta_d < 1$ is the maximum fractional thickness change due to pulsating blood flow, t is time and f is the blood pulse frequency in Hz.

**[00103]** The HbO2 attenuation coefficient should also be considered a time-dependent value as it is related to blood oxygenation levels in the patient, thus dependent on the proportions of oxy- and deoxy-hemoglobin in arterial blood. In practice, however, the variation of blood oxygenation will generally be on a much longer time scale than the variations due to the patient's pulse. Strong and sudden variations of blood oxygenation are rare and indicative of a serious health condition that is unlikely to be encountered in the normal operation of the IAN sensor. Nevertheless, monitoring of blood oxygenation with a pulse oxymeter is considered a good practice in the utilization of such a sensor, if only as a check point for the sensor's calibration, as detailed below. For the sake of the proposed model, the attenuation coefficient was however assumed to be a constant.

**[00104]** Combining Equs. (2)-(4), the model was built to provide an order of magnitude for the optical signal intensity over time to be expected from such an approach. The resulting output optical power is described with:

**[00105]** $$I(t) = I_0 \exp\left[-\left\{p(\mu_{marrow} - \mu_{cortical}) + \mu_{cortical}\right\}d_{total} - \mu_{HbO2} d_{HbO2-baseline}(1 + \Delta_d \cos(2\pi f t))\right] \quad (5).$$

**[00106]** The near infrared spectroscopy (NIRS) based sensor goal is to measure the thickness $d_{total}$ of trabecular bone tissue between the probe (or drill) tip and the neurovascular bundle containing the IAN. In one embodiment, a lock-in amplifier may be used to establish the magnitude of the oscillating signal and circumvent the DC signal that is influenced by the static trabecular tissue, as detailed below. In one embodiment, a typical method is to use the root-mean square value of the AC signal:

**[00107]** $$I_{RMS} = \sqrt{\langle I^2(t) \rangle} \quad (6),$$

**[00108]** where:

**[00109]** $$\langle I^2(t) \rangle = \int_0^{1/f} t[I(t)]^2 dt \quad (7).$$

**[00110]** Solving Equ. (6) from (5) and (7) and using a Taylor expansion for the exponential function up to the second degree in the integral leads to:

**[00111]** $$I_{RMS} \approx \left[ \sqrt{2} I_0 \frac{1}{2f} \sqrt{1 + B^2 \Delta_d^2} \right] e^{-Kd_{total}+B};$$
$$B = \mu_{HbO2} d_{HbO2-baseline}; \quad (8),$$
$$K = p(\mu_{marrow} - \mu_{cortical}) + \mu_{cortical}$$

**[00112]** and thus,

$$d_{total} \approx \left\{ \mu_{HbO2} d_{HbO2-baseline} - \ln\left( \sqrt{2} f \left( \frac{I_{RMS}}{I_0} \right) \frac{1}{\sqrt{1 + (\Delta_d \mu_{HbO2} d_{HbO2-baseline})^2}} \right) \right\} \frac{1}{p(\mu_{marrow} - \mu_{cortical}) + \mu_{cortical}} \quad (9).$$

**[00113]** With such a model, assuming an input of 10 mW of optical power at the proper wavelength, an output signal of approximately 0.07 mW would be produced.

**[00114]** FIG. 7 shows a spectral absorption probe system **300** for evaluating proximity to an artery **302**, according to the above detailed technique and according to one embodiment. The probe system **300** comprises a light source **304** for generating excitation light **306** having a wavelength adapted for absorption by blood chromophores, an excitation optical fiber **308** to bring the excitation light **306** near the artery **302** and a collection optical fiber **310** for capturing back-scattered light from the artery **302**. The probe system **300** comprises a light detector **312** operatively connected to the collection optical fiber **310** and a signal processor

**314** operatively connected to the light detector **312** for determining a distance **320** to the artery **302** based on the back-scattered light and on Beer-Lambert law of light absorption using a value for surrounding tissue attenuation coefficient (μeff).

**[00115]** FIG. 18 illustrates a spectral absorption probe method for evaluating proximity to an artery, according to one embodiment. According to processing step **1810**, an excitation light having a wavelength adapted for absorption by blood chromophores is generated. According to processing step **1820**, the excitation light is brought near the artery. According to processing step **1830**, back-scattered light is captured from the artery. According to processing step **1840**, the back-scattered light from the artery is processed for determining a distance to the artery based on Beer-Lambert law of light absorption using a value for surrounding tissue attenuation coefficient (μeff).

**[00116]** As anatomically the artery is part of the IAN bundle, locating it is almost equivalent to locating the nerve. This approach can be implemented in a similar package as the LCI / OCT fiber probe that can fit within the dental drill bit. The blood pulse can be used to eliminate all background signals via AC-coupling of the detector or lock-in amplification. The signal amplitude can then be used to assess the distance from the probe to the IAN bundle based on Beer-Lambert's law. A calibration process is however typically required before use *in situ* due to patient's tissues variability of optical properties. Notably, the approach relies on the absorption of oxyhemoglobin, which itself will potentially vary according to blood oxygen saturation. As such, the approach might benefit from the probe being used in conjunction with a pulse oxymeter that would monitor oxygen saturation levels and thus, indirectly account for variations of the blood attenuation coefficient. A variation on this approach uses the same spectral principle as the pulse oxymeter, utilizing two wavelengths (typically, 660 nm to target deoxyhemoglobin and 850 nm to target oxyhemoglobin, but generally comprised between 650 nm and 900 nm), as shown in FIG. 6 which illustrates a drill-integrated IAN sensor **600** based on the NIR spectral absorption technique. As detailed therein, distance can be obtained by isolating the distance variable (d) in Equ. 1, but requires that the surrounding tissues' attenuation coefficient (μeff) be known through a calibration step. It has to be noted that such a technique would be limited in the precision of the measurement, as the signal output results from probing a large volume with diffused photons and is thus inherently averaging over that

volume, which might skew the output value of distance. Using AC-coupling and a proper calibration is key in this approach, as detailed thereafter.

**[00117]** In one embodiment, the calibration for the spectral absorption technique may be integrated within the standard configuration if a lock-in amplifier (not shown) is used. In such an embodiment, as illustrated in FIG. 8, an intensity-modulated light excitation of modulation frequency f (typ. ~100 MHz range) and modulation depth M1 propagating in the tissues will suffer phase retardation and reduction of the modulation depth as a function of the attenuation properties of the traversed medium. The retrieved signal has the same frequency as the incident one, but due to absorption and scattering in the medium, it suffers a phase shift $\Delta\Phi$ and an attenuation of the modulation depth M2 relative to the incident signal. The change in phase $\Delta\Phi$ and modulation depth $\Delta M$ is correlated to the average attenuation coefficient and can be used to extract the parameter $\mu_{eff}$ in Equ. 1. This method is known in the art of Diffuse Optical Tomography. To achieve accurate results, though, the modulation frequency should be in the range of about 100 MHz to 500 MHz. Unfortunately, limitations in current lock-in amplifier electronics make most affordable conventional devices to operate up to the hundreds of kHz range.

**[00118]** This issue can be solved by using a heterodyning processing circuit before the lock-in amplifier input, as illustrated in FIG. 9, using signal mixing with an intermediate frequency and using principles of Amplitude Modulation to extract the difference signal. In the illustrated embodiment of a probe system **400**, the light source **402** is driven at high frequency with a light source driver **404**, for example at 200 MHz, to insure adequate resolution on the extracted values $\Delta\Phi$ and $\Delta M$. A local oscillator **406** generates a slightly larger frequency, larger by 50 kHz as a non-limitative example. The oscillator **406** and the driver **404** are phase-locked by a PLL circuit **408**. Mixing those two signals produces the sum and difference signals (amplitude modulation) and a low-pass filter **410** is used to retain only the difference component. The detection channel **412** operates similarly and a standard, low-bandwidth dual-phase lock-in amplifier **414** can then be used.

**[00119]** Furthermore, it is known in the art that the positioning of the probe for calibration (in contact or not with tissues and other variants) can skew the calibration measurement. The

method might thus need an additional step where the instrument is pre-calibrated with an appropriate optical phantom (not shown) with known attenuation properties supplied with the device, before the in-patient calibration step. This way, a relative value to the phantom properties would be obtained and should be enough for the proper operation of the sensor.

**[00120]** With such an approach, the calibration of the device for the patient's jaw tissues may be made at the beginning or at an early phase of the drilling process by the surgeon, before enabling the sensor, which is of great advantage.

**[00121] Embodiments and possible features of the Optical IAN Sensor**

**[00122]** Different embodiments of the Optical IAN probe system can be envisioned for both approaches described above. The following is a short description of each of the potential embodiments and implementations envisioned:

**[00123] Standalone self-contained spectral absorption-based fiber-probe**: FIG. 10A shows an embodiment wherein the sensor is built as a standalone fiber optic device **500** contained within a biocompatible metallic rod **502**. The rod **502** contains two optical fibers **504**, **506** (single- or multimode) along its axial direction. One fiber serves to bring the excitation light within the tissues while the other captures the back-scattered light. Fibers **504**, **506** run parallel to each other and are separated by an adequate distance (1-2 mm) to fit into the hole bored by the dental drill bit (typ. 2 mm dia.). The skilled addressee will appreciate that the separation between the two fibers **504**, **506** should be as large as possible to maximize penetration depth. Indeed, in back-reflected diffuse optical sensing, the depth of penetration is increased with source-detector separation. The skilled addressee will also appreciate that multimode fibers may be employed to increase light throughput in both channels. In this embodiment, the fiber probe itself is connected to the device back-end. As previously mentioned, the excitation fiber is connected to a light source (either LED, laser or other source) or multiple light sources each having an appropriate wavelength for optimized absorption by blood chromophores (mainly oxy- and deoxyhemoglobin). Typical wavelengths are around 660 nm and 850 nm. The light source output could be modulated at a reference frequency in the kHz range. The collection fiber is connected to an appropriate light detector such as a photodiode, an avalanche photodiode (APD), a photomultiplier tube (PMT), a

camera or the like. The detector output signal is either AC-coupled or connected to a lock-in amplifier operating at the same reference frequency as the light source modulation. The goal of the modulation signal or the AC-coupling is to reject background signals coming from other tissues than the flowing arterial blood. A variation of this embodiment makes use of a varying input optical power into the tissue to establish the neurovascular bundle position relative to the probe based on an intensity threshold approach, where larger input powers will statistically increase linearly the number of photons reaching larger depths, thus improving the chance of detecting some of these photons that might probe the neurovascular bundle.

**[00124]** **Standalone self-contained low coherence interferometry-based fiber-probe**: FIG. 10B shows another embodiment similar to the one shown in FIG. 10A in shape but implementing the OCT approach. As illustrated, a single fiber **508** can be used for illumination and collection purposes. Due to the difference in requirements between OCT and the spectral absorption concept, the fiber probe should be made of one or multiple single-mode optical fibers to prevent detrimental dispersion and spatial propagation modes mixing, according to one embodiment. The back-end of the probe utilizes classical OCT configurations, such as time-domain-based, frequency-domain OCT or swept-source-based implementations, as previously detailed. In this embodiment, the back-end is entirely fiberized and uses fiber couplers to connect with the probe itself, as is well-known in the art. In a further embodiment, the probe forward-looking configuration can be implemented for B-mode scanning, by integrating a proximal scanning system installed in the back-end coupled to a bundle of single mode optical fibers, or through a distal scanning mechanism integrated into the probe head itself that would use one single-mode optical fiber.

**[00125]** **Drill-integrated probe**: Referring again to FIG. 6, any of the described embodiments can be integrated at the center of the drill bit **610** of a dental surgery drill. The center of a dental drill bit **610** can have a hollow core **602** to allow for cooling water to circulate down to the drilling site **604**. The fiber probe can be inserted within this hollow core **602**.

**[00126]** **Combined OCT / Spectral absorption probe**: Such a combined configuration uses the advantages of each approach. The spectral absorption approach has potentially a

greater detection range, while the OCT approach is more straightforward and offer potentially better resolution at short range. A combined sensor probe could thus potentially identify roughly the position of the IAN bundle at a distance with the spectral absorption mode and then switch to an OCT approach when close to the IAN (typ. within 1.5 mm). The sensor construction would require two or three optical fibers grouped in a bundle. A single-mode fiber would bring the excitation light. A second single-mode fiber would be used for OCT light collection, while a third multimode fiber would be used for the spectral absorption mode light collection channel. Alternatively, the single-mode excitation fiber could double-up as the collection fiber for the OCT technique.

**[00127] Spectral absorption fiber probe with disjointed source and collection channels:** FIG. 11 shows an embodiment of a disjointed spectral absorption IAN sensor **700**. In this configuration of the spectral absorption technique, one or multiple excitation optical fibers **702** are positioned on the side of the gum or jawbone **704**, outside of the probe handpiece **706** itself (or the drill bit), while the detection optical fiber **708** is still integrated in the probe handpiece **706**, within the drilling hole **710** in the bone **704**. Such a configuration allows larger separation of the source and collection channels, which will increase depth sensitivity of the technique. Indeed, as previously mentioned, in back-reflected diffuse optical sensing, the depth of penetration is increased with source-detector separation. Alternatively, the source and collection channels can be reversed, with the detection being done laterally on the gum and the illumination being integrated in the drill bit, or probe handpiece. In a further embodiment, using multiple optical fibers built in a linear array may provide refined measurements of the neurovascular bundle's position in the jaw.

**[00128] Use of a double-clad optical fiber:** FIG. 12 illustrates a double-clad optical fiber-based IAN sensor handpiece **800** which may be used alternatively to the use of two optical fibers in the probe. The core **802** of the double-clad optical fiber **804** is used as the excitation channel to send light into tissues and the first cladding **806** acts as the collection channel. In the OCT approach and in one embodiment, the core **802** is built for single mode propagation. The first clad **806** will typically have a large numerical aperture, making it ideal for light collection. The second clad **808** insure proper waveguide behavior for the first clad **806**. This approach would benefit especially the OCT technique as the separation between core and first

cladding would probably be too low for efficient implementation of the spectral absorption technique.

**[00129] Combining the spectral absorption probe with a pulse oxymeter in the technique:** FIG. 13 shows a spectral absorption-based IAN sensor apparatus **900** that uses an entirely separate pulse oxymeter **902** operatively connected to a finger **904** of the patient as a monitor of blood oxygenation variations over the course of the drilling procedure, to maintain an inline calibration of the arterial blood absorption properties. In other words, this embodiment enables to compensate variations of blood optical properties from the oxygenation levels variation ($\Delta$SatO2) to provide more accurate distance measurements, by updating the device calibration factors in real-time. Indeed, large variations in the optical properties will skew the sensor distance measurement. That being said, normal individuals will generally not see variations in blood oxygenation larger than ~2%, which might well be within the error bar of the distance measurement.

**[00130] Developing a B-mode OCT technique using the drill rotation for scanning:** FIG. 14 shows a IAN sensor **1000** using a conical scanning principle that uses the drill rotation and a beveled double-clad optical waveguide **1002** that rotates with the drill **1004** in such a way that the source and collection channels would observe the tissues in front of the drill tip slightly off-axis. As it should become apparent to the skilled addressee, this is an alternative implementation to the standard B-mode scanning technique that operates along a line in the transverse plane. The drill rotation would allow a ring in the transverse plane to be scanned along the light propagation axis, essentially probing a conical surface within the jaw. The IAN bundle would intersect this conical surface at two opposite locations. The signal processor (not shown) of the device **1000** could then create an image **1006** by "unfolding" the conical surface on a computer screen **1008**, giving the dental surgeon a high resolution image similar to an ultrasonogram in real-time. The advantage of this B-mode scanning method is that the IAN bundle orientation in the transverse plane relative to the drill axis can be arbitrary. In the other implementations described, the IAN bundle should lie on the drilling axis, or the axis of the forward looking probe, to be detected properly. Otherwise the drill bit might pass beside the nerve and still produce damage, because the sensor did not "see" the

IAN bundle. Note that with the NIR spectral absorption technique, this flaw is fairly reduced due to the volume averaging effect mentioned earlier.

**[00131] Implement Doppler OCT in the probe and use tissue changes or movement as a contrast mechanism:** In addition to using standard OCT in the sensor, this configuration uses the Doppler effect to lock on blood flow. Doppler OCT is generally used to measure quantitatively microvasculature blood flow. In the case of this sensor, a qualitative measurement is enough to locate the IAN bundle. As such, the implementation of Doppler measurements in the OCT device would be simpler and cheaper. Experiments were conducted with Doppler OCT on an ex vivo human jawbone piece from which the neurovascular bundle was removed and a tube containing a flowing scattering fluid was connected, imitating blood flow in the canal. Results have shown that using the Doppler Effect as part of the spectral absorption technique might benefit the device.

**[00132]** According to another embodiment, another variant of OCT data processing that utilizes changes or movement in the tissue like Doppler OCT, namely speckle variance OCT [Refs: A. Mariampillai et al., Opt. Lett. 33(13), 1530 (2008) ; A. Mariampillai et al., Opt. Lett. 35(8), 1257 (2010)], can be used to embody the sensor. It proceeds as follow: first, a series of B-mode images of the same sample section over time is acquired. Second, for each pixel location the average value and variance are computed using pixel value of all images at that same exact location. This process leads to two 2D images. The first one is made with the pixel average value. Therefore, non-zero pixels in that image are those associated with a stationary/non-moving part of the sample. The second image is made with the pixel variance values. Thus, non-zero pixels in that image are associated with the moving/spatially-varying part of the sample. In a similar fashion to Doppler OCT, this kind of processing will lead to contrast generation between hard and soft tissues in movement, or contrast based on tissue "viscosity". Results have shown that the fluid may be identified from the variance image, contrasting with the bone section. This method could potentially make good usage of blood flow in the neurovascular bundle.

**[00133] Use of a non-specific vascular contrast agent to facilitate artery detection:** A vascular contrast agent, such as Indocyanine Green which is a NIR fluorescent dye approved

for clinical use in a number of indications, can be used to enhance the signal coming from the artery in the IAN bundle. Injection of a bolus of ICG into the systemic circulation will momentarily make the artery in the IAN bundle fluoresce at 830 nm (when excited at 780 nm) against a non-fluorescent background, increasing the overall contrast dramatically. If tuned to the fluorescent wavelength, the spectral absorption sensor technique will have a much easier time at spotting the IAN bundle. The modulated excitation would equally translate to a modulated fluorescence signal. A difficulty is however that the device needs to be calibrated at two wavelengths (780 and 830 nm) instead of one. This can be solved by adding a second light source and operating in the same manner as described above for calibration at the two wavelengths, before the ICG injection.

**[00134]** In similar fashion, the various embodiments based on LCI / OCT can benefit from the potential application of optical clearing agents at the site of probing. Biocompatible optical clearing agents, such as fructose, glycerol, propylene glycol, glucose or mannitol solutions can partially replace the interstitial fluid due to hyperosmotic properties and provide a refractive index matching medium that reduces scattering due to a number of cell structures and organelles, thus increasing the transparency of the tissues to optical wavelengths and improving the depth penetration.

**[00135] Dental Drill integration of the Optical IAN Sensor**

**[00136]** Integration of the sensor into a drill bit presents a number of mechanical challenges, the most important ones being the rotation speed and how to protect the optical sensor at the drill tip, without blocking light injection and detection. Dental drills can rotate at rates up to 20,000 RPM. In typical use for dental implant surgery, the rotation speed will be in the range of 2,000 to 4,000 RPM.

**[00137]** To fit within the hollow core of a drill bit, the optical fiber assembly should be secured in such a way that the optical fibers do not come into contact with the rotating inner wall. The friction at high rotating speeds would most certainly break the optical fibers. An alternative is to have the fiber assembly rotate with the drill bit, so that relative positioning of the fibers and the inner wall is stationary. FIG. 15A shows a drill-integrated IAN sensor **1100**

rotating with the drill bit **1102** and using an optical fiber rotary joint **1104** for coupling the optical fibers in the drill head.

**[00138]** FIG. 15B illustrates another alternative drill integrated IAN sensor **1150** wherein a rod-like optical waveguide **1152** is built as an integral part of the drill bit **1154** with a non-contact optical coupler **1156** from the optical fibers **1158** coming from the back-end in the drill head. The skilled addressee will note that having a rotating handpiece requires that the probe design have circular symmetry, which is not achievable with a two-fiber design as the one shown in FIG. 10A. In this last case, the handpiece should remain stationary with the drill bit rotating around the sensing assembly, as previously detailed.

**[00139]** In a further embodiment, in order to prevent introduction of organic tissues and debris within the hollow core that could clog it and prevent proper function of the sensor, the tip of the drill bit may be plugged with a hard and transparent material (not shown), so it can withstand the large frictions of the drilling process while allowing light to pass through. Diamond or zirconium crystals would potentially be the best materials, due to their exceptional hardness and transparency in the visible and NIR spectral window but the skilled addressee will appreciate that other arrangements may be considered.

**[00140] Extensions of the technology to other applications**

**[00141]** The described invention could also be used in other fields of surgery where proximity to a neurovascular bundle embedded in hard tissues, such as bone, must be assessed during a surgical activity such as drilling or cutting. It can also be used to identify the presence of voids inside tissue structures, such as sinus cavities in the cranial anatomy, during drilling procedures. As another example of application, a LCI / OCT-based probe could also be envisioned as a bone mapping tool in oral surgery to determine the gums thickness at specific locations, as long as the device detection range is sufficient.

**[00142]** The embodiments described above are intended to be exemplary only. The scope of the invention is therefore intended to be limited solely by the appended claims.

## CLAIMS

1. A spectral absorption probe system for evaluating proximity to an artery, comprising:

a light source for generating excitation light having a wavelength adapted for absorption by blood chromophores;

an excitation optical fiber to bring said excitation light near the artery;

a collection optical fiber for capturing back-scattered light from said artery;

a light detector operatively connected to said collection optical fiber; and

a signal processor operatively connected to said light detector for determining a distance to said artery based on said back-scattered light and on Beer-Lambert law of light absorption using a value for surrounding tissue attenuation coefficient (μeff).

2. The spectral absorption probe system as claimed in claim 1, further comprising a biocompatible metallic rod surrounding said excitation optical fiber and said collection optical fiber.

3. The spectral absorption probe system as claimed in claim 1, wherein said excitation optical fiber and said collection optical fiber are provided in a single double-clad optical fiber with a fiber core of said double-clad optical fiber bringing said excitation light near said artery and a first clad of said double-clad optical fiber capturing said back-scattered light from said artery.

4. The spectral absorption probe system as claimed in any one of claims 1 to 3, wherein said probe system is fibered and integrated within a hollow core of a drill bit.

5. The spectral absorption probe system as claimed in any one of claims 1 to 4, wherein an operating depth range of the probe system is comprised between 1 mm and 5 mm.

6. The spectral absorption probe system as claimed in any one of claims 1 to 5, wherein the light source is selected from a group consisting of a LED, a laser and a set of light source units.

7. The spectral absorption probe system as claimed in any one of claims 1 to 6, wherein the wavelength of the light source is comprised between 650 nm and 900 nm.

8. The spectral absorption probe system as claimed in any one of claims 1 to 7, further comprising an additional light source having a wavelength adapted for absorption by blood chromophores, the wavelengths of the light source and of the additional light source being each comprised between 650 nm and 900 nm.

9. The spectral absorption probe system as claimed in any one of claims 1 to 8, wherein the light detector is selected from a group consisting of a photodiode, an avalanche photodiode (APD), a photomultiplier tube (PMT) and a camera.

10. The spectral absorption probe system as claimed in any one of claims 1 to 9, further comprising a calibration unit having a pulse oxymeter for monitoring oxygen saturation levels to maintain an inline calibration of arterial blood absorption properties.

11. The spectral absorption probe system as claimed in any one of claims 1 to 10, wherein said surrounding tissue attenuation coefficient (μeff) is determined according to absorption and scattering in surrounding tissue of a calibration excitation signal.

12. The spectral absorption probe system as claimed in any one of claims 1 to 11, wherein the signal processor comprises a lock-in amplifier and a heterodyning processing circuit connected thereto.

13. The spectral absorption probe system as claimed in any one of claims 1 to 12, wherein the light detector is AC-coupled to the signal processor.

14. The spectral absorption probe system as claimed in any one of claims 1 to 13, wherein the excitation optical fiber and the collection optical fiber are separated from each other and extend angularly.

15. The spectral absorption probe system as claimed in claim 14, wherein a single one of said excitation optical fiber and said collection optical fiber is integrated within a hollow core of a drill bit.

16. A spectral absorption and low coherence interferometry probe system for evaluating proximity to a tissue layer, comprising:

a light source for generating excitation light having at least one wavelength adapted for absorption by blood chromophores and low coherence;

an excitation optical fiber to bring said excitation light near the tissue layer;

a collection optical fiber for capturing back-scattered light from said tissue layer;

a light detector operatively connected to said collection optical fiber;

a digital signal processor operatively connected to said light detector for determining a distance to said tissue layer based on said back-scattered light and on Beer-Lambert law of light absorption using a value for surrounding tissue attenuation coefficient (μeff);

a low coherence interferometry sub-system operatively connected to the excitation optical fiber and the collection optical fiber and having a beam splitter and a reference mirror; and

a signal processor operatively connected to said low coherence interferometry sub-system for evaluating a distance to said tissue layer based on said back-scattered light received by said collection optical fiber.

17. The spectral absorption and low coherence interferometry probe system as claimed in claim 16, wherein the excitation optical fiber comprises a single mode fiber and further wherein the collection optical fiber comprises a single mode fiber for OCT mode light collection and a multimode fiber for spectral absorption mode light collection.

18. The spectral absorption and low coherence interferometry probe system as claimed in any one of claims 16 and 17, wherein the probe system comprises a forward-looking transverse scanner enabling B-mode imaging.

19. A spectral absorption probe method for evaluating proximity to an artery, comprising:

generating an excitation light having a wavelength adapted for absorption by blood chromophores;

bringing said excitation light near the artery;

capturing back-scattered light from said artery; and

processing said back-scattered light from said artery for determining a distance to said artery based on Beer-Lambert law of light absorption using a value for surrounding tissue attenuation coefficient (μeff).

20. The spectral absorption probe method as claimed in claim 19 for evaluating proximity to an inferior alveolar nerve in situ.

21. The spectral absorption probe method as claimed in any one of claims 19 and 20, further comprising monitoring oxygen saturation levels to maintain an inline calibration of arterial blood absorption properties.

22. The spectral absorption probe method as claimed in any one of claims 19 to 21, further comprising determining said surrounding tissue attenuation coefficient (μeff) according to absorption and scattering in surrounding tissue of a calibration excitation signal.

23. The spectral absorption probe method as claimed in any one of claims 19 to 22, wherein said back-scattered light is captured angularly and at a given distance with respect to said brought excitation light.

24. The spectral absorption probe method as claimed in any one of claims 19 to 23, further comprising using a vascular contrast agent.

25. A spectral absorption and low coherence interferometry probe method for evaluating proximity to a tissue layer, comprising:

generating an excitation light having at least one wavelength adapted for absorption by blood chromophores and low coherence;

bringing said excitation light near the tissue layer;

capturing back-scattered light from said tissue layer;

processing said back-scattered light for determining a first distance to said tissue layer based on Beer-Lambert law of light absorption using a value for surrounding tissue attenuation coefficient (μeff);

performing interferometry between said low coherence excitation light and said back-scattered light for providing an interference signal; and

processing said interference signal for evaluating a second distance to said tissue layer.

26. A low coherence interferometry probe system for evaluating proximity to a tissue layer, comprising:

a low coherence light source for generating low coherence excitation light;

an excitation optical fiber to bring said low coherence excitation light near the tissue layer;

a collection optical fiber for capturing back-scattered light from said tissue layer;

a low coherence interferometry sub-system operatively connected to the excitation optical fiber and the collection optical fiber and having a beam splitter and a reference mirror; and

a digital signal processor operatively connected to said low coherence interferometry sub-system for evaluating a distance to said tissue layer based on said back-scattered light received by said collection optical fiber.

27. The low coherence interferometry probe system as claimed in claim 26, wherein said tissue layer is selected from a group consisting of a canal wall, an artery, a nerve, a neurovascular bundle and a sinus floor.

28. The low coherence interferometry probe system as claimed in any one of claims 26 to 27, wherein said probe system is fibered and is integrated within a hollow core of a drill bit.

29. The low coherence interferometry probe system as claimed in any one of claims 26 to 28, wherein the low coherence light source is selected from a group consisting of a superluminescent LED, a pulsed laser and a frequency-swept laser source.

30. The low coherence interferometry probe system as claimed in any one of claims 26 to 29, wherein an operating depth range of the probe system is comprised between 1 mm and 5 mm.

31. The low coherence interferometry probe system as claimed in any one of claims 26 to 30, wherein the excitation optical fiber and the collection optical fiber are both embedded in a single-mode optical fiber.

32. The low coherence interferometry probe system as claimed in any one of claims 26 to 31, wherein the excitation optical fiber and the collection optical fiber are provided in a single double-clad optical fiber having a core acting as an excitation channel, an inner clad acting as a collection channel and an outer clad surrounding the inner cladding.

33. The low coherence interferometry probe system as claimed in any one of claims 26 to 32, wherein the probe system is operated in A-mode.

34. The low coherence interferometry probe system as claimed in any one of claims 26 to 33, wherein the probe system comprises a forward-looking transverse scanner enabling B-mode imaging.

35. The low coherence interferometry probe system as claimed in any one of claims 26 to 34, wherein the excitation optical fiber and the collection optical fiber are both embedded in a rotating beveled double-clad optical fiber having a core acting as an excitation channel, an inner cladding acting as a collection channel and an outer cladding surrounding the inner cladding, the probe system being operated in a B-mode providing conical imaging.

36. The low coherence interferometry probe system as claimed in any one of claims 26 to 35, further comprising at least one of a Doppler OCT unit for performing Doppler measurements and a speckle variance OCT unit.

37. A low coherence interferometry probe method for evaluating proximity to a tissue layer, comprising:

generating a low coherence excitation light;

bringing said low coherence excitation light near the tissue layer;

capturing back-scattered light from said tissue layer;

performing interferometry between said low coherence excitation light and said back-scattered light for providing an interference signal; and

processing said interference signal for evaluating a distance to said tissue layer.

38. The low coherence interferometry probe method as claimed in claim 37 for evaluating proximity to an inferior alveolar nerve in situ.

39. The low coherence interferometry probe method as claimed in any one of claims 37 to 38, wherein the probe method is operated according to A-mode.

40. The low coherence interferometry probe method as claimed in any one of claims 37 to 39, further comprising forward-looking transverse scanning of the tissue layer for enabling B-mode imaging.

41. The low coherence interferometry probe method as claimed in any one of claims 37 to 40, further comprising using an optical clearing agent at a probing site.

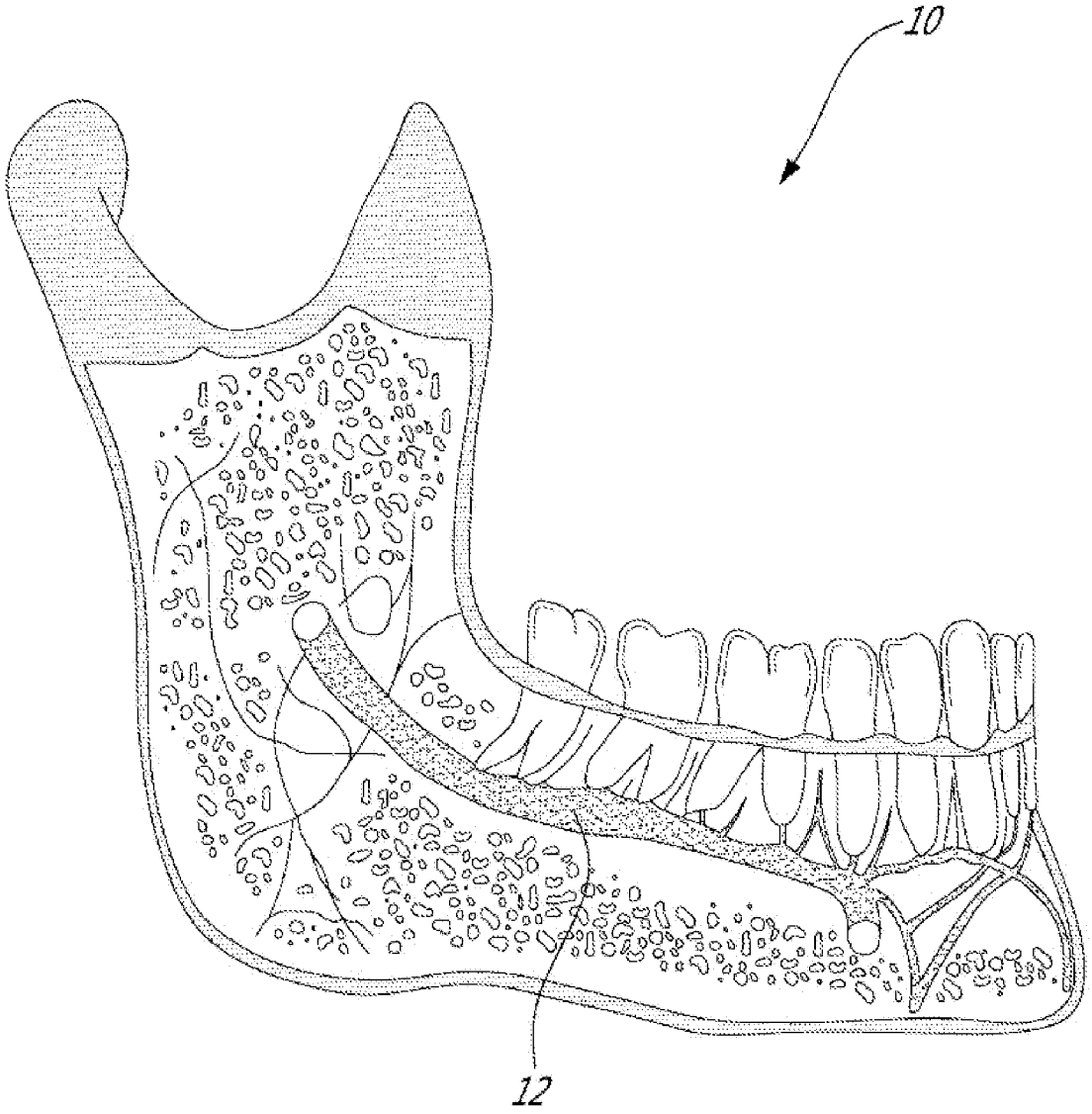


FIG. 1

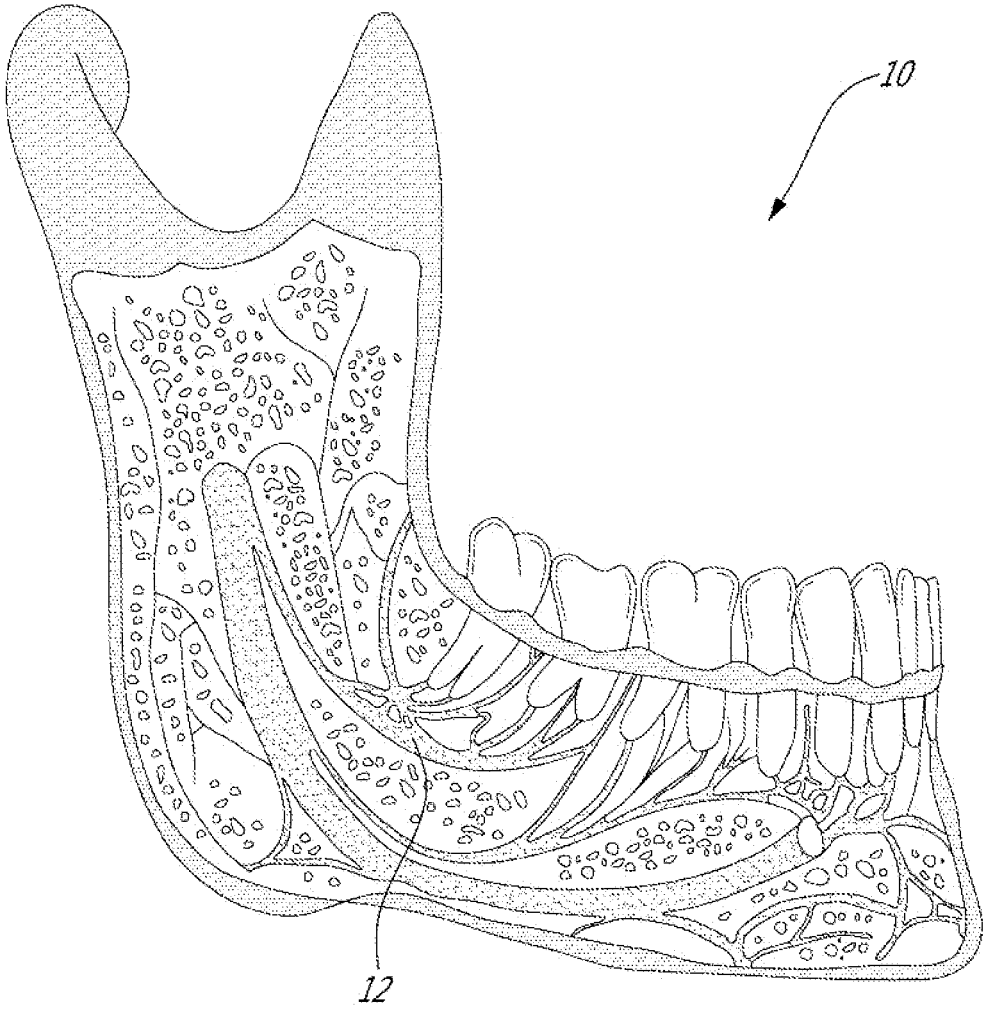


FIG. 2

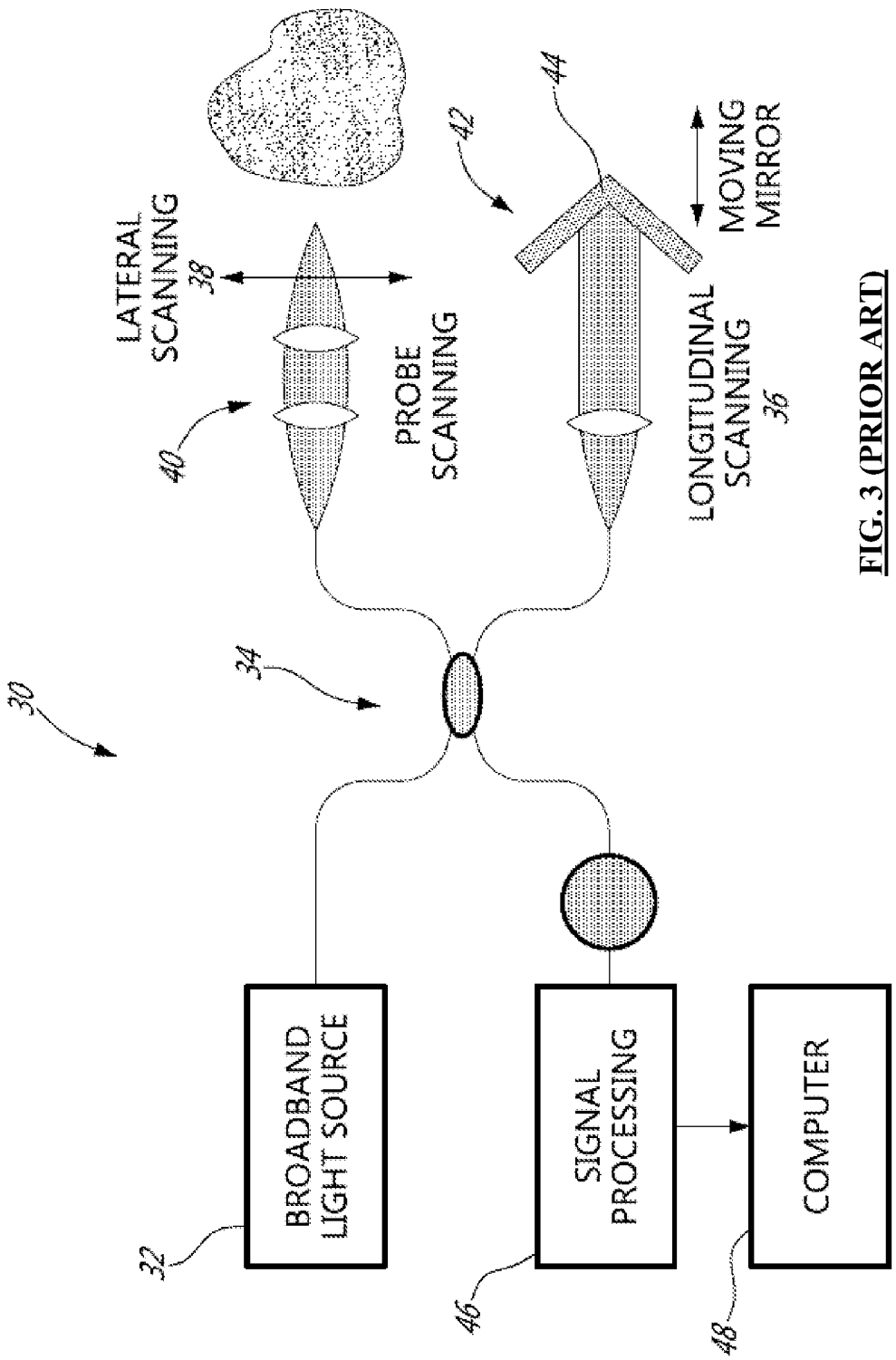


FIG. 3 (PRIOR ART)

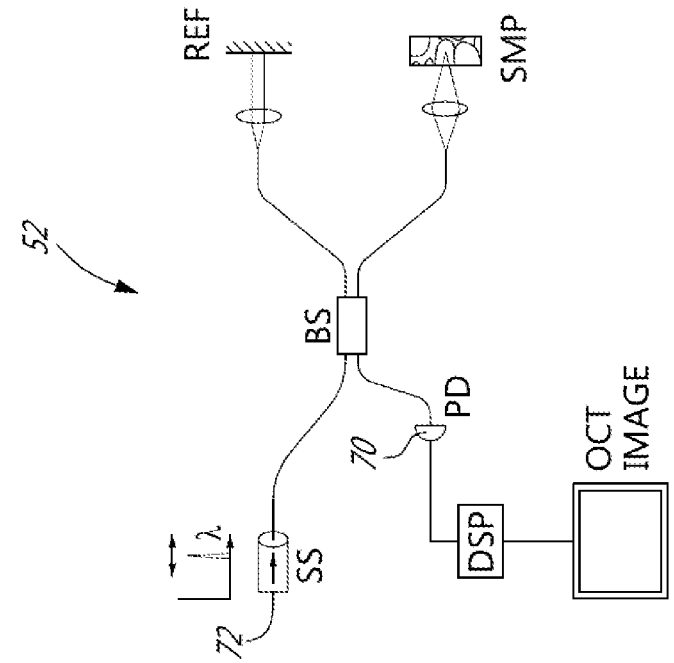


FIG. 4B (PRIOR ART)

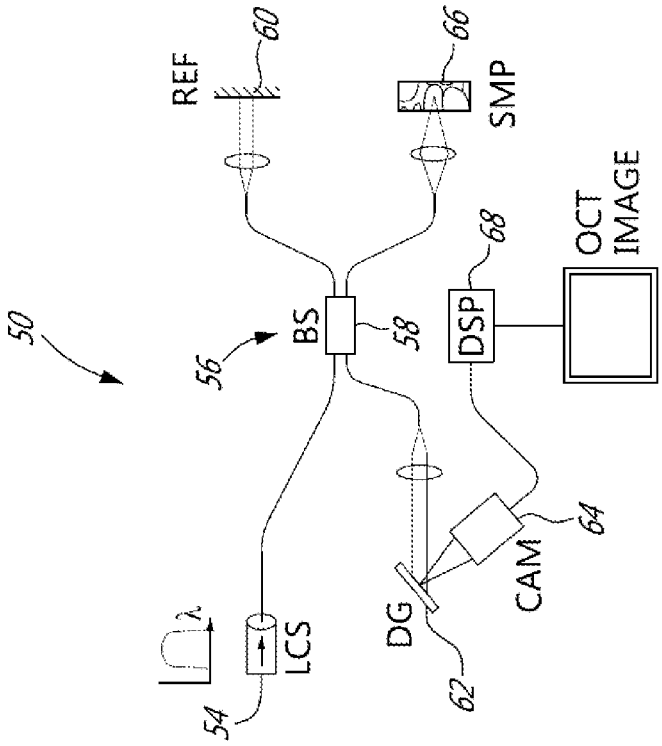


FIG. 4A (PRIOR ART)

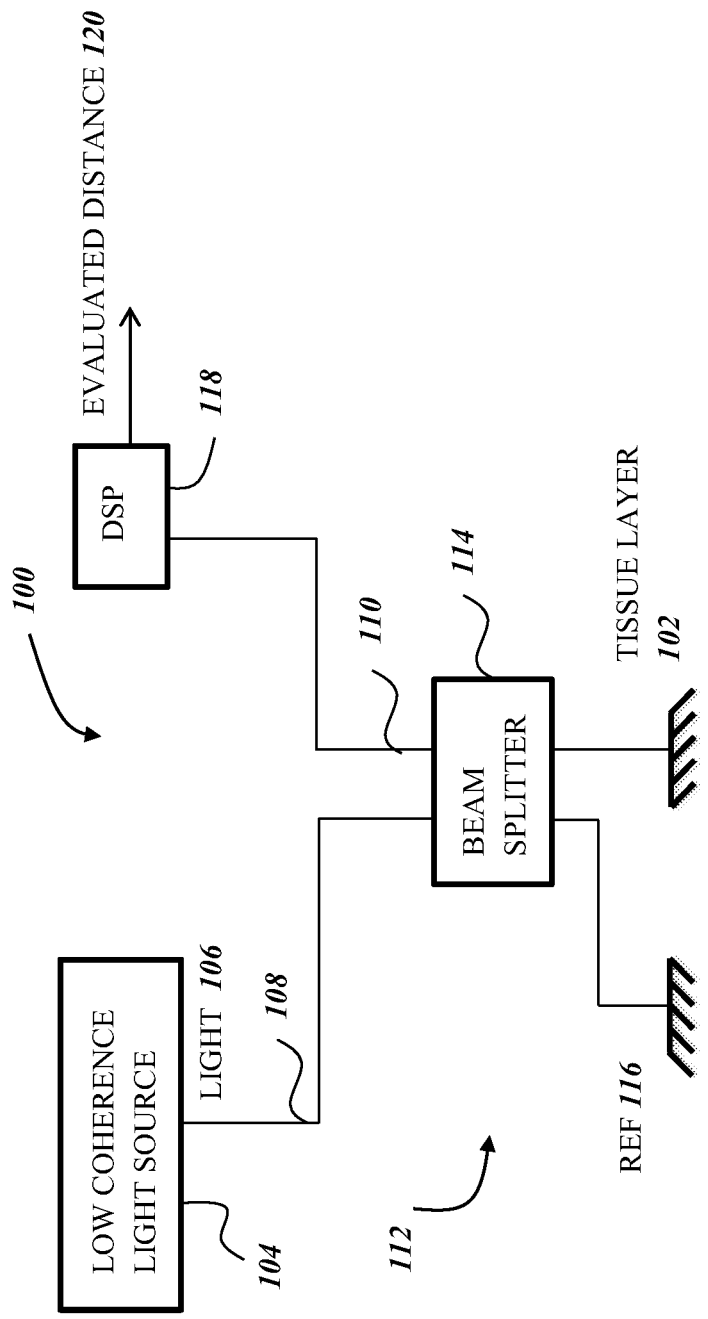
EVALUATED DISTANCE 120
DSP
118
100
110
114
TISSUE LAYER
102
BEAM SPLITTER
LOW COHERENCE LIGHT SOURCE
LIGHT 106
108
104
112
REF 116

FIG. 5

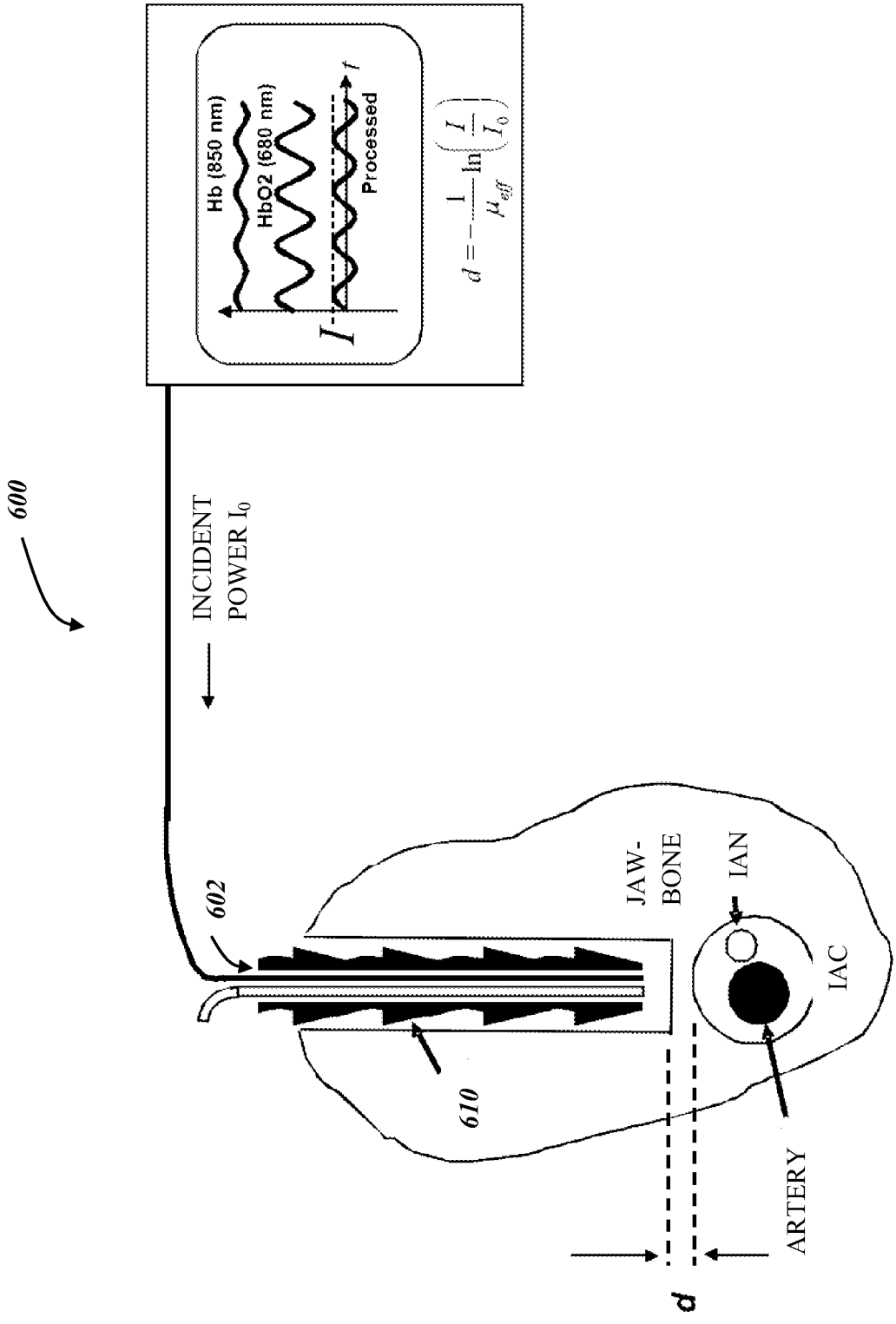
600
INCIDENT
POWER $I_0$
Hb (850 nm)
HbO2 (680 nm)
Processed
I
t
$d = -\frac{1}{\mu_{eff}} \ln\left(\frac{I}{I_0}\right)$
602
610
JAW-
BONE
IAN
IAC
ARTERY
d

FIG. 6

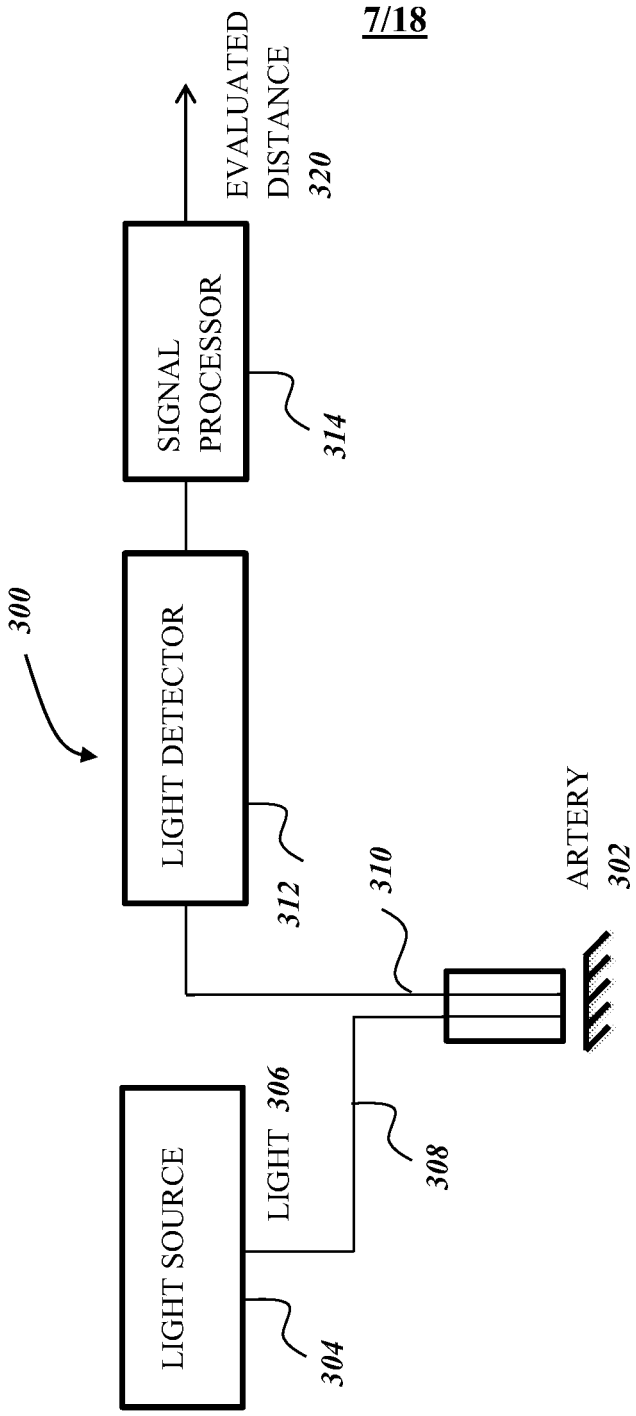
300
LIGHT SOURCE
304
LIGHT 306
308
LIGHT DETECTOR
312
310
ARTERY
302
SIGNAL PROCESSOR
314
EVALUATED DISTANCE
320

FIG. 7

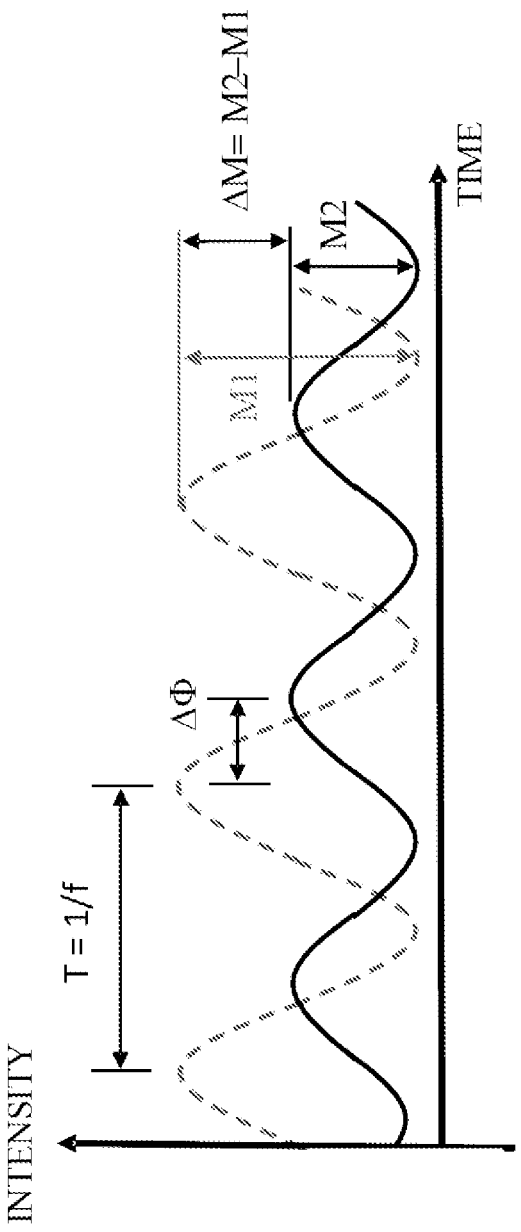


FIG. 8

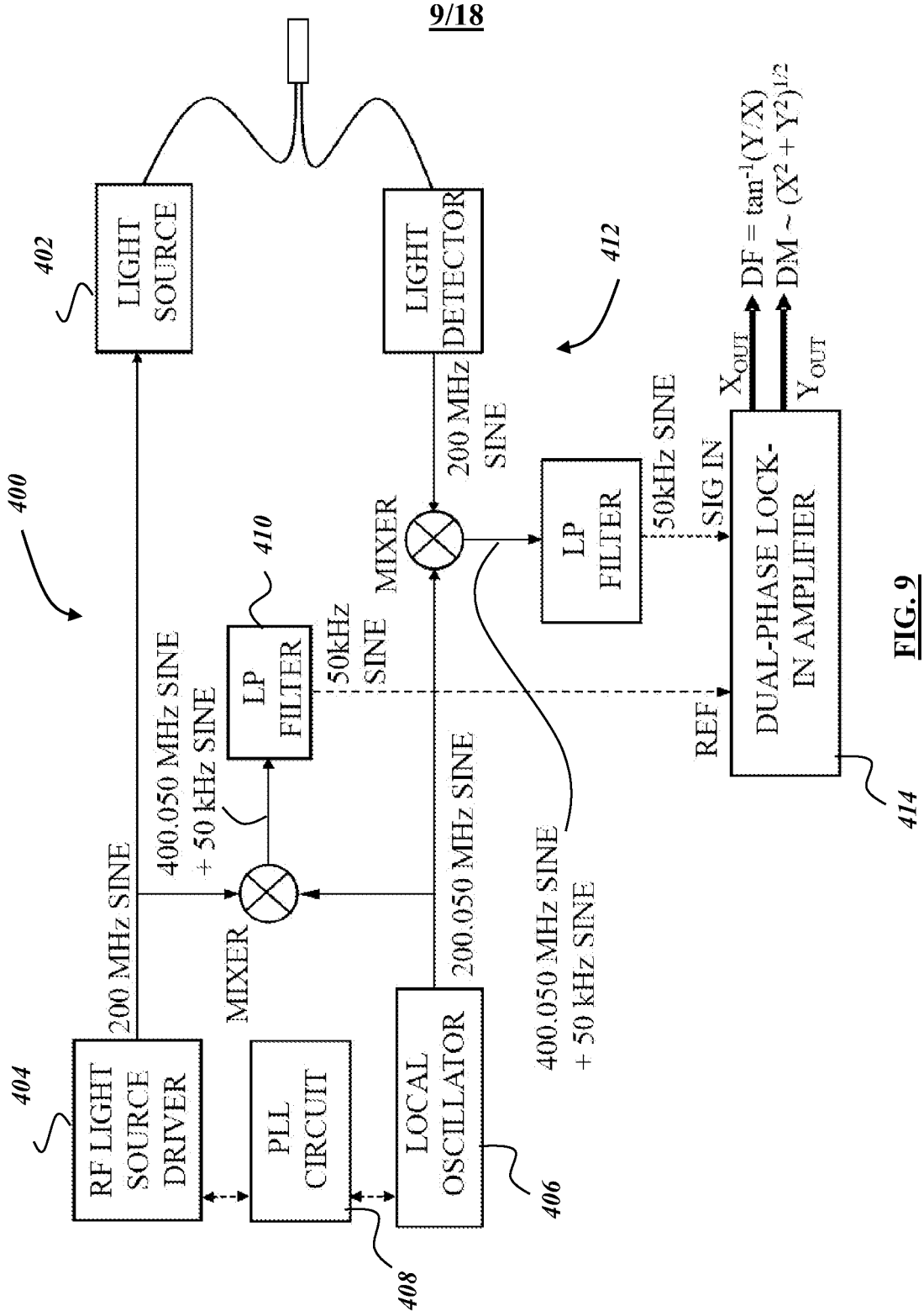
400
402
LIGHT SOURCE
LIGHT DETECTOR
412
200 MHz SINE
MIXER
LP FILTER
50kHz SINE
SIG IN
DF = tan-1(Y/X)
DM ~ (X2 + Y2)1/2
XOUT
YOUT
410
50kHz SINE
REF
DUAL-PHASE LOCK-IN AMPLIFIER
414
400.050 MHz SINE + 50 kHz SINE
200 MHz SINE
MIXER
200.050 MHz SINE
400.050 MHz SINE + 50 kHz SINE
404
RF LIGHT SOURCE DRIVER
PLL CIRCUIT
LOCAL OSCILLATOR
406
408

FIG. 9

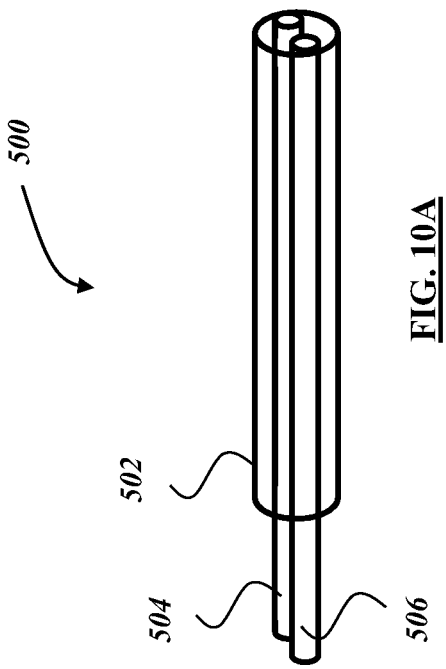


FIG. 10A

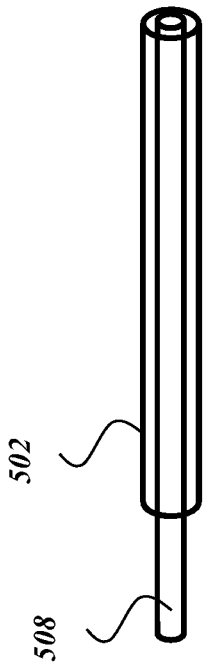


FIG. 10B

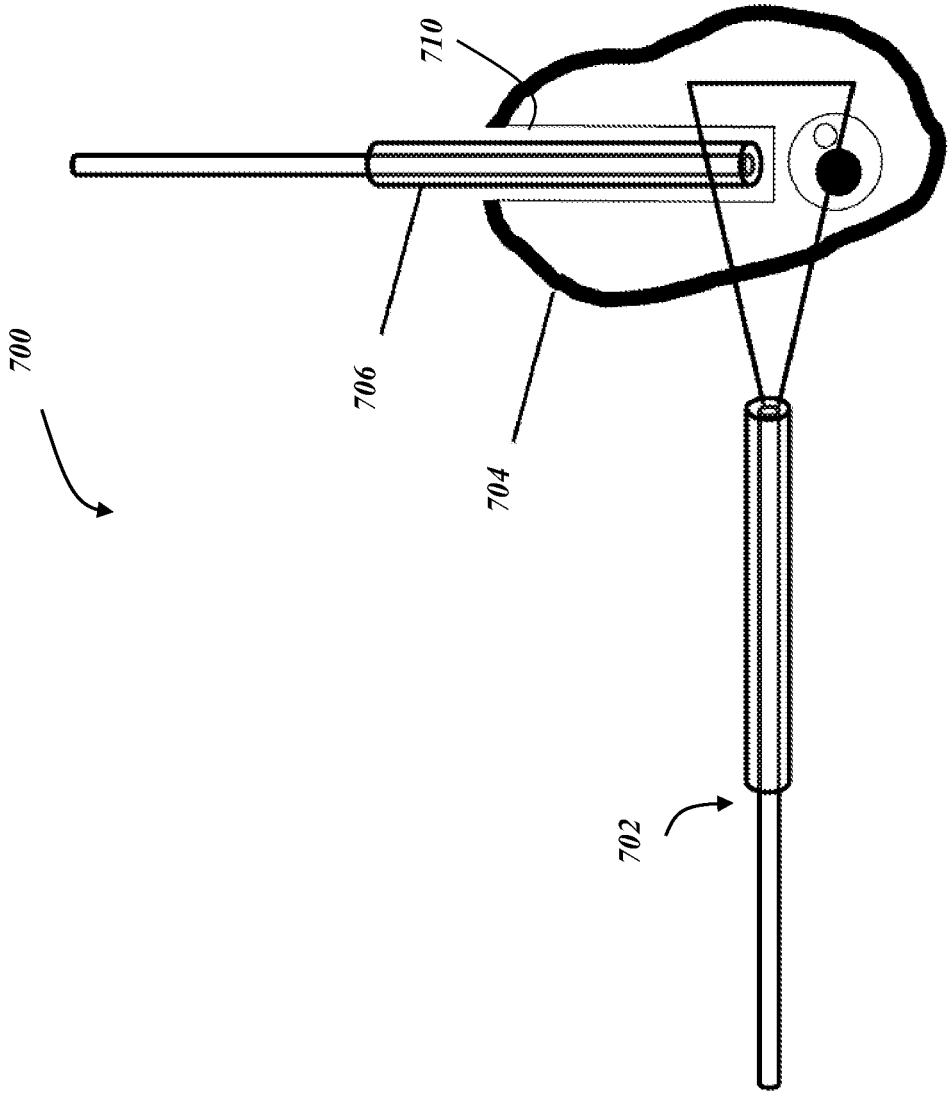


FIG. 11

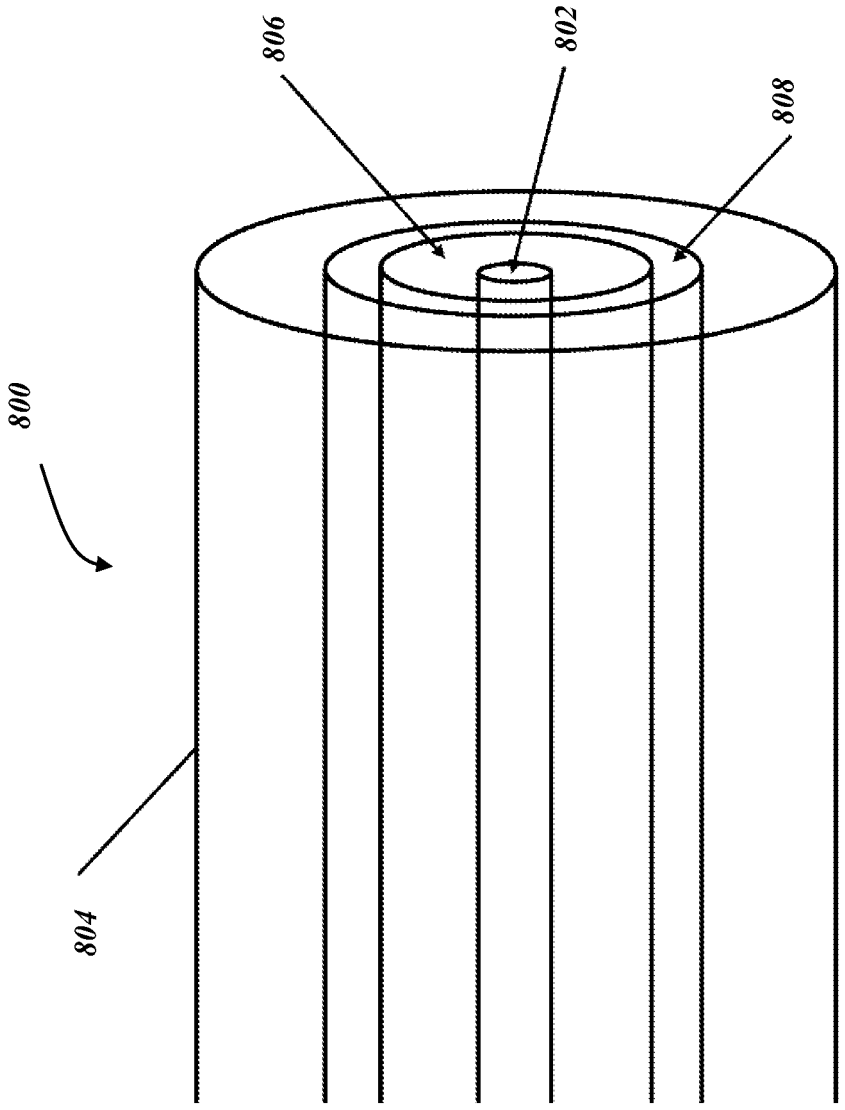


FIG. 12

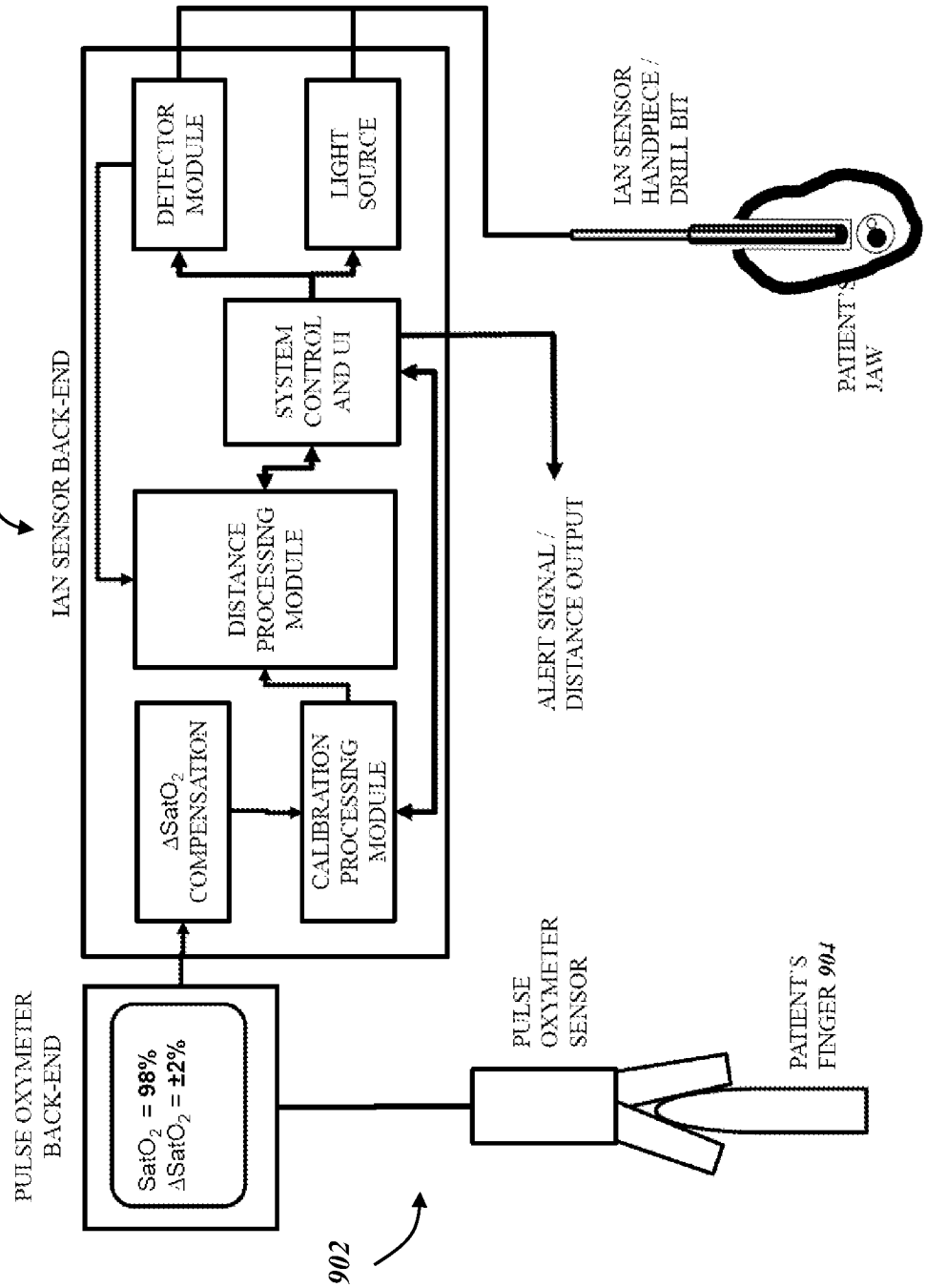
900
IAN SENSOR BACK-END
DETECTOR MODULE
LIGHT SOURCE
IAN SENSOR HANDPIECE / DRILL BIT
SYSTEM CONTROL AND UI
PATIENT'S JAW
DISTANCE PROCESSING MODULE
ALERT SIGNAL / DISTANCE OUTPUT
ΔSatO2 COMPENSATION
CALIBRATION PROCESSING MODULE
PULSE OXYMETER BACK-END
SatO2 = 98%
ΔSatO2 = ±2%
PULSE OXYMETER SENSOR
PATIENT'S FINGER 904
902

FIG. 13

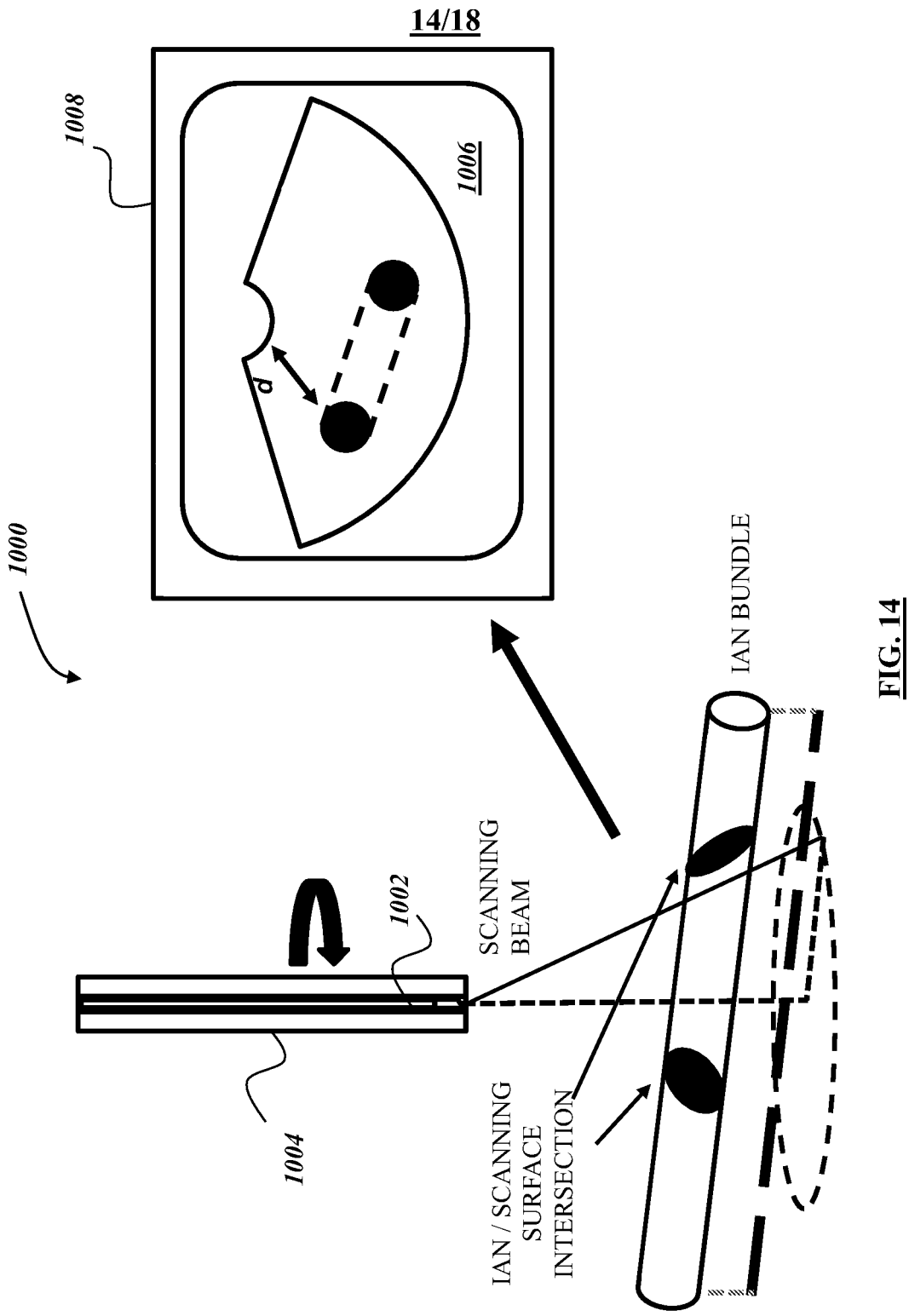
1000
1008
1006
d
1002
1004
SCANNING BEAM
IAN / SCANNING SURFACE INTERSECTION
IAN BUNDLE

FIG. 14

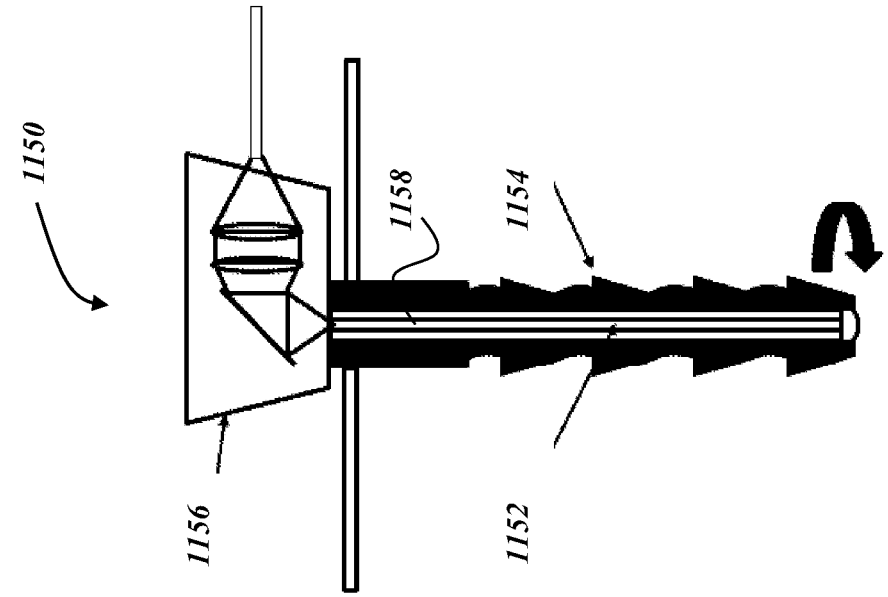


FIG. 15B

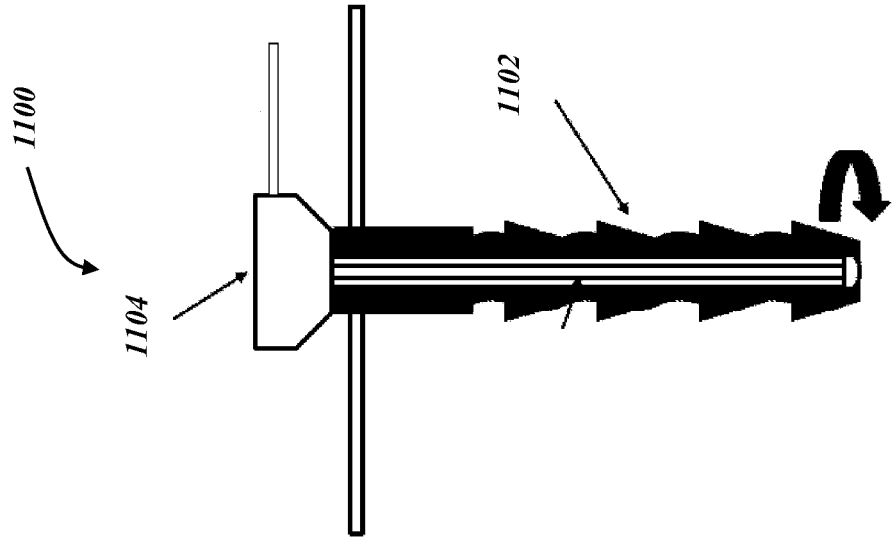


FIG. 15A

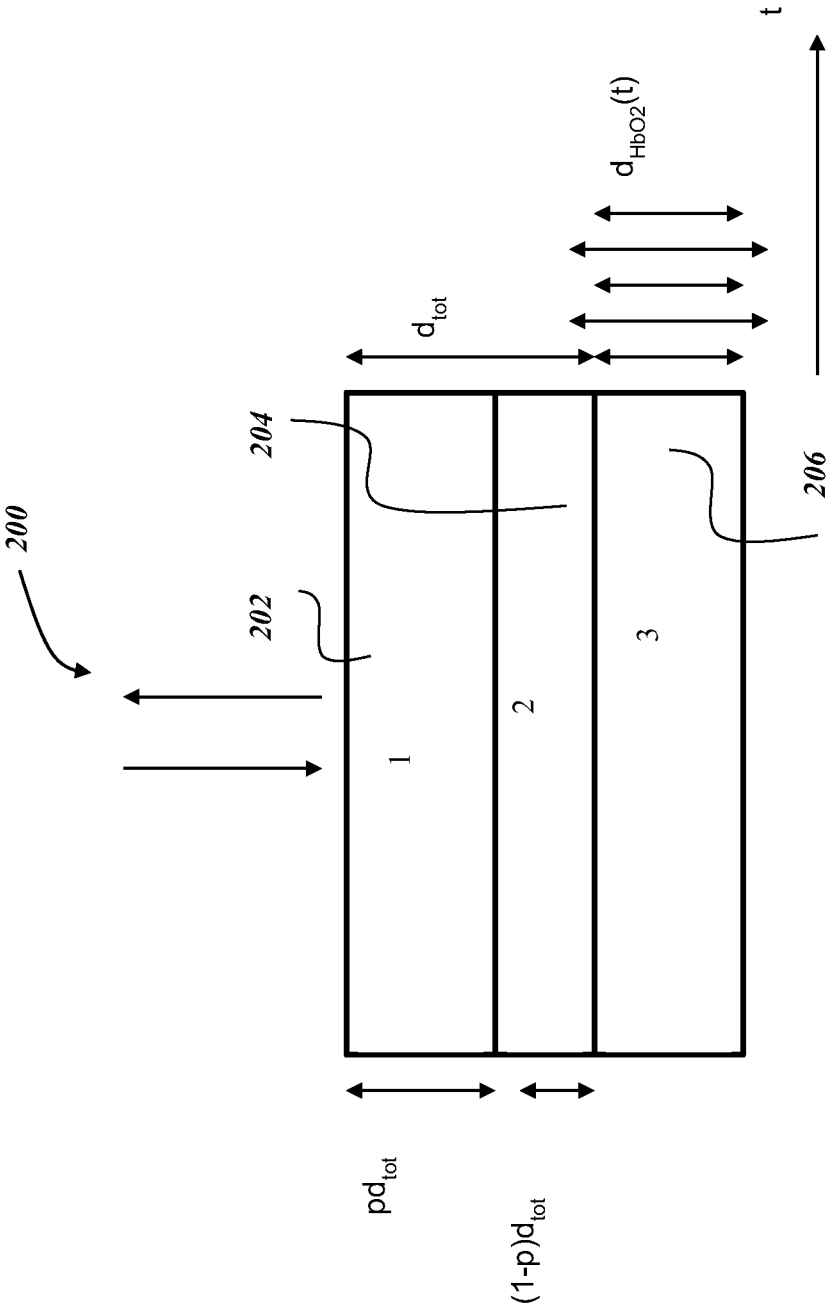


FIG. 16

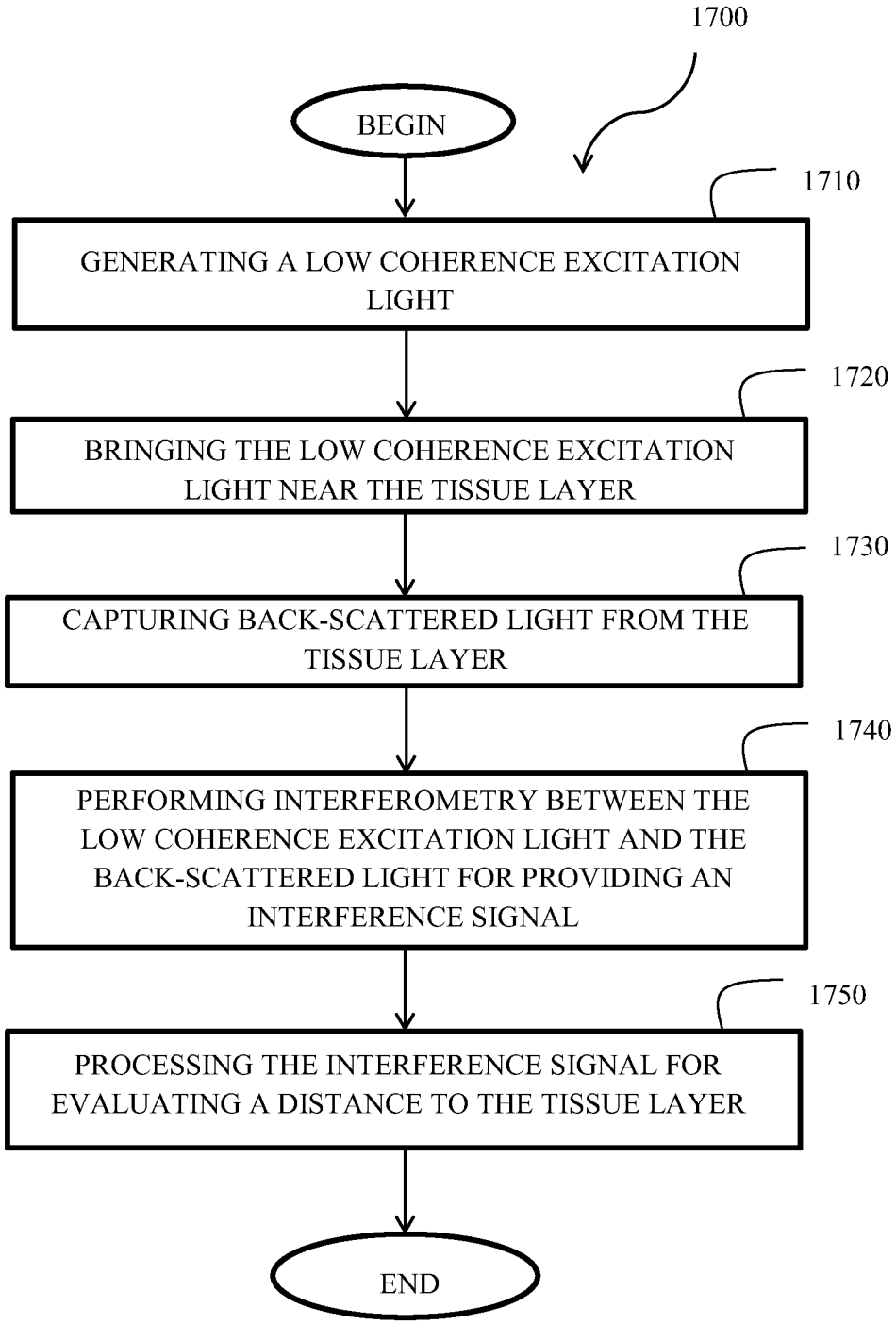
1700
BEGIN
1710
GENERATING A LOW COHERENCE EXCITATION LIGHT
1720
BRINGING THE LOW COHERENCE EXCITATION LIGHT NEAR THE TISSUE LAYER
1730
CAPTURING BACK-SCATTERED LIGHT FROM THE TISSUE LAYER
1740
PERFORMING INTERFEROMETRY BETWEEN THE LOW COHERENCE EXCITATION LIGHT AND THE BACK-SCATTERED LIGHT FOR PROVIDING AN INTERFERENCE SIGNAL
1750
PROCESSING THE INTERFERENCE SIGNAL FOR EVALUATING A DISTANCE TO THE TISSUE LAYER
END

FIG. 17

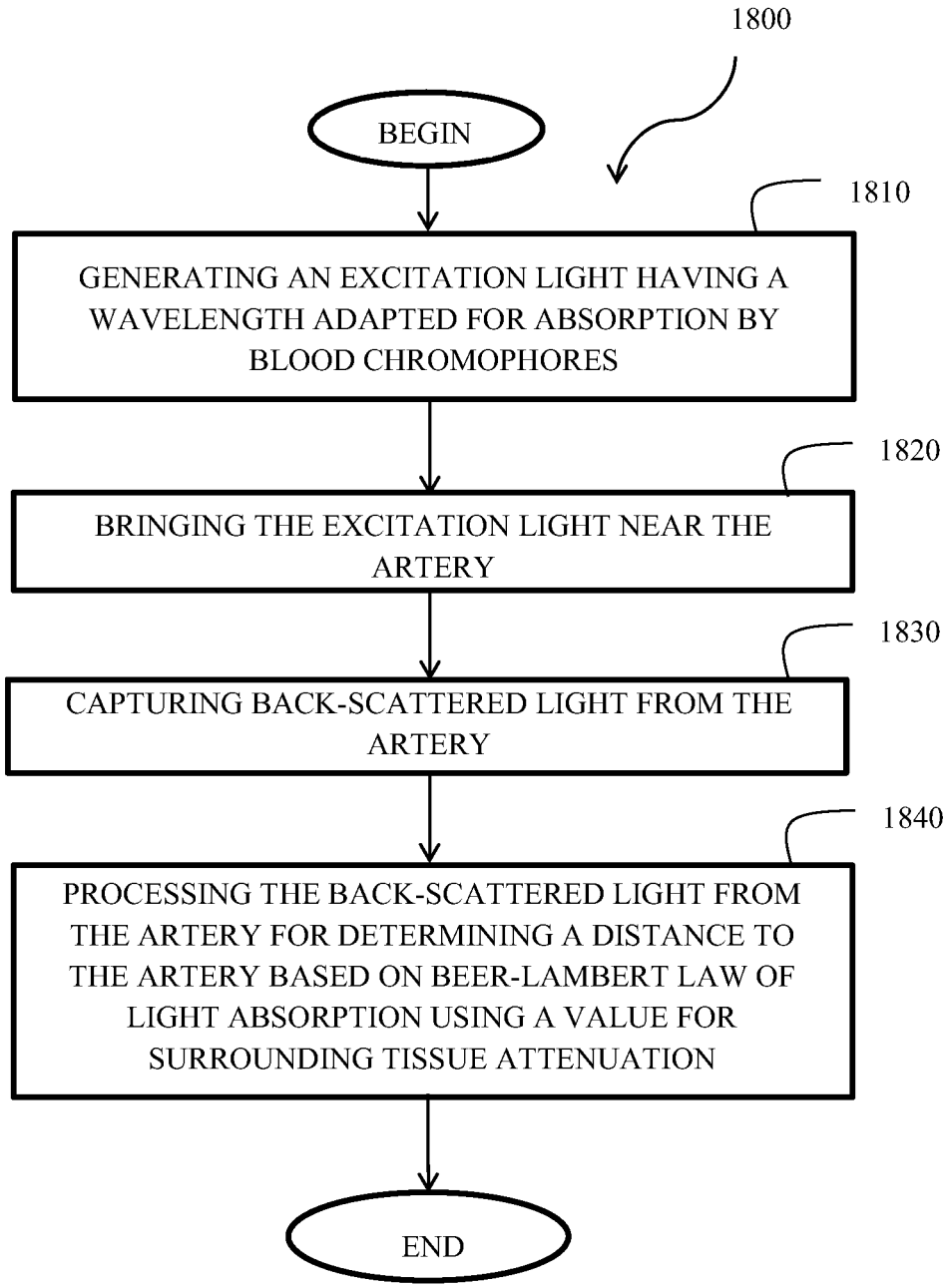
1800
BEGIN
1810
GENERATING AN EXCITATION LIGHT HAVING A WAVELENGTH ADAPTED FOR ABSORPTION BY BLOOD CHROMOPHORES
1820
BRINGING THE EXCITATION LIGHT NEAR THE ARTERY
1830
CAPTURING BACK-SCATTERED LIGHT FROM THE ARTERY
1840
PROCESSING THE BACK-SCATTERED LIGHT FROM THE ARTERY FOR DETERMINING A DISTANCE TO THE ARTERY BASED ON BEER-LAMBERT LAW OF LIGHT ABSORPTION USING A VALUE FOR SURROUNDING TISSUE ATTENUATION
END

FIG. 18

# INTERNATIONAL SEARCH REPORT

International application No.
PCT/IB2012/050045

A. CLASSIFICATION OF SUBJECT MATTER
IPC: ***A61B 6/14*** (2006.01) , ***A61C 8/00*** (2006.01)
According to International Patent Classification (IPC) or to both national classification and IPC

B. FIELDS SEARCHED

Minimum documentation searched (classification system followed by classification symbols)
IPC (2006): A61B (in combination with keywords)

Documentation searched other than minimum documentation to the extent that such documents are included in the fields searched

Electronic database(s) consulted during the international search (name of database(s) and, where practicable, search terms used)
Database: TotalPatent, Canadian Patent Database (Intellect), EPOQUE (EPODOC), USPTO West, IEEE Xplore
Keywords: spectral, absorb, probe, artery, blood, scatter, implant, Beer Lambert, tissue, attenuation, coefficient, backscatter

C. DOCUMENTS CONSIDERED TO BE RELEVANT

| Category* | Citation of document, with indication, where appropriate, of the relevant passages | Relevant to claim No. |
|---|---|---|
| Y | US 6564087 (PITRIS et al.) 13 May 2003 (13-05-2003)<br>* Column 2, lines 5-40 and 55-60; column 3, lines 5-19; column 3, line 56 to column 4, line 6; column 6, line 5 to column 7, line 60; column 12, line 31 to column 13, line 2; column 17, line 34 to column 18, line 53; column 20, line 55 to column 21, line 6; column 22, lines 17-24 * | 1-3, 5-8, 11-14, 16-20, 22, 23, 25-27 and 29-40 |
| Y | US 2005/0151976 (TOMA) 14 July 2005 (14-07-2005)<br>* Paragraphs [0012], [0033], [0034], [0040], [0041] * | 1-3, 5-8, 11-14, 16-20, 22, 23, 25-27 and 29-40 |
| A | US 6134003 (TEARNEY et al.) 17 October 2000 (17-10-2000) | 1-41 |
| A | US 6485413 (BOPPART et al.) 26 November 2002 (26-11-2002) | 1-41 |
| A | US 2010/0280392 (LIU et al.) 4 November 2010 (-04-11-2010) | 1-41 |
| A | US 2001/0047137 (MORENO et al.) 29 November 2001 (29-11-2001) | 1-41 |

[ ] Further documents are listed in the continuation of Box C.

[X] See patent family annex.

* Special categories of cited documents :

"A" document defining the general state of the art which is not considered to be of particular relevance

"E" earlier application or patent but published on or after the international filing date

"L" document which may throw doubts on priority claim(s) or which is cited to establish the publication date of another citation or other special reason (as specified)

"O" document referring to an oral disclosure, use, exhibition or other means

"P" document published prior to the international filing date but later than the priority date claimed

"T" later document published after the international filing date or priority date and not in conflict with the application but cited to understand the principle or theory underlying the invention

"X" document of particular relevance; the claimed invention cannot be considered novel or cannot be considered to involve an inventive step when the document is taken alone

"Y" document of particular relevance; the claimed invention cannot be considered to involve an inventive step when the document is combined with one or more other such documents, such combination being obvious to a person skilled in the art

"&" document member of the same patent family

| Date of the actual completion of the international search | Date of mailing of the international search report |
|---|---|
| 29 March 2012 (29-03-2012) | 23 April 2012 (23-04-2012) |

| Name and mailing address of the ISA/CA | Authorized officer |
|---|---|
| Canadian Intellectual Property Office<br>Place du Portage I, C114 - 1st Floor, Box PCT<br>50 Victoria Street<br>Gatineau, Quebec K1A 0C9<br>Facsimile No.: 001-819-953-2476 | Alan Chan (819) 934-7888 |

**INTERNATIONAL SEARCH REPORT**
Information on patent family members

International application No.
PCT/IB2012/050045

| Patent Document Cited in Search Report | Publication Date | Patent Family Member(s) | Publication Date |
|---|---|---|---|
| US6564087B1 | 13 May 2003 (13-05-2003) | AU1977597A | 16 September 1997 (16-09-1997) |
| | | CA2289598A1 | 19 November 1998 (19-11-1998) |
| | | CA2289598C | 20 July 2004 (20-07-2004) |
| | | DE69227902D1 | 28 January 1999 (28-01-1999) |
| | | DE69227902T2 | 17 June 1999 (17-06-1999) |
| | | DE69227902T3 | 22 April 2010 (22-04-2010) |
| | | DE69738291D1 | 27 December 2007 (27-12-2007) |
| | | DE69738291T2 | 11 September 2008 (11-09-2008) |
| | | DE69821610D1 | 18 March 2004 (18-03-2004) |
| | | DE69821610T2 | 23 December 2004 (23-12-2004) |
| | | EP0581871A1 | 09 February 1994 (09-02-1994) |
| | | EP0581871A4 | 27 April 1994 (27-04-1994) |
| | | EP0581871B1 | 16 December 1998 (16-12-1998) |
| | | EP0581871B2 | 12 August 2009 (12-08-2009) |
| | | EP0883793A1 | 16 December 1998 (16-12-1998) |
| | | EP0883793B1 | 14 November 2007 (14-11-2007) |
| | | EP0971626A1 | 19 January 2000 (19-01-2000) |
| | | EP0981733A1 | 01 March 2000 (01-03-2000) |
| | | EP0981733B1 | 11 February 2004 (11-02-2004) |
| | | JPH06511312A | 15 December 1994 (15-12-1994) |
| | | JP3479069B2 | 15 December 2003 (15-12-2003) |
| | | JP2000503237A | 21 March 2000 (21-03-2000) |
| | | JP3628026B2 | 09 March 2005 (09-03-2005) |
| | | JP2004105708A | 08 April 2004 (08-04-2004) |
| | | JP3692131B2 | 07 September 2005 (07-09-2005) |
| | | JP2001527659A | 25 December 2001 (25-12-2001) |
| | | JP4065963B2 | 26 March 2008 (26-03-2008) |
| | | JP2001515382A | 18 September 2001 (18-09-2001) |
| | | JP2002214127A | 31 July 2002 (31-07-2002) |
| | | US5321501A | 14 June 1994 (14-06-1994) |
| | | US5459570A | 17 October 1995 (17-10-1995) |
| | | US5465147A | 07 November 1995 (07-11-1995) |
| | | US5748598A | 05 May 1998 (05-05-1998) |
| | | US5784352A | 21 July 1998 (21-07-1998) |
| | | US5956355A | 21 September 1999 (21-09-1999) |
| | | US6111645A | 29 August 2000 (29-08-2000) |
| | | US6134003A | 17 October 2000 (17-10-2000) |
| | | US6160826A | 12 December 2000 (12-12-2000) |
| | | US6282011B1 | 28 August 2001 (28-08-2001) |
| | | US2001036002A1 | 01 November 2001 (01-11-2001) |
| | | US6421164B2 | 16 July 2002 (16-07-2002) |
| | | US6485413B1 | 26 November 2002 (26-11-2002) |
| | | US6501551B1 | 31 December 2002 (31-12-2002) |
| | | WO0042906A2 | 27 July 2000 (27-07-2000) |
| | | WO0042906A3 | 11 January 2001 (11-01-2001) |
| | | WO0042906B1 | 01 March 2001 (01-03-2001) |
| | | WO9219930A1 | 12 November 1992 (12-11-1992) |
| | | WO9533970A1 | 14 December 1995 (14-12-1995) |
| | | WO9533971A1 | 14 December 1995 (14-12-1995) |
| | | WO9701167A1 | 09 January 1997 (09-01-1997) |
| | | WO9723870A1 | 03 July 1997 (03-07-1997) |
| | | WO9732182A1 | 04 September 1997 (04-09-1997) |
| | | WO9835203A2 | 13 August 1998 (13-08-1998) |
| | | WO9835203A3 | 29 October 1998 (29-10-1998) |
| | | WO9838907A1 | 11 September 1998 (11-09-1998) |
| | | WO9852021A1 | 19 November 1998 (19-11-1998) |
| US2005151976A1 | 14 July 2005 (14-07-2005) | US2005151976A1 | 14 July 2005 (14-07-2005) |
| | | WO2005058154A1 | 30 June 2005 (30-06-2005) |

Continued in Supplemental Box

Patent family members continued

| | | | |
|---|---|---|---|
| US6134003A | 17 October 2000 (17-10-2000) | AU1977597A | 16 September 1997 (16-09-1997) |
| | | CA2289598A1 | 19 November 1998 (19-11-1998) |
| | | CA2289598C | 20 July 2004 (20-07-2004) |
| | | DE69227902D1 | 28 January 1999 (28-01-1999) |
| | | DE69227902T2 | 17 June 1999 (17-06-1999) |
| | | DE69227902T3 | 22 April 2010 (22-04-2010) |
| | | DE69738291D1 | 27 December 2007 (27-12-2007) |
| | | DE69738291T2 | 11 September 2008 (11-09-2008) |
| | | DE69821610D1 | 18 March 2004 (18-03-2004) |
| | | DE69821610T2 | 23 December 2004 (23-12-2004) |
| | | EP0581871A1 | 09 February 1994 (09-02-1994) |
| | | EP0581871A4 | 27 April 1994 (27-04-1994) |
| | | EP0581871B1 | 16 December 1998 (16-12-1998) |
| | | EP0581871B2 | 12 August 2009 (12-08-2009) |
| | | EP0883793A1 | 16 December 1998 (16-12-1998) |
| | | EP0883793B1 | 14 November 2007 (14-11-2007) |
| | | EP0971626A1 | 19 January 2000 (19-01-2000) |
| | | EP0981733A1 | 01 March 2000 (01-03-2000) |
| | | EP0981733B1 | 11 February 2004 (11-02-2004) |
| | | JPH06511312A | 15 December 1994 (15-12-1994) |
| | | JP3479069B2 | 15 December 2003 (15-12-2003) |
| | | JP2000503237A | 21 March 2000 (21-03-2000) |
| | | JP3628026B2 | 09 March 2005 (09-03-2005) |
| | | JP2004105708A | 08 April 2004 (08-04-2004) |
| | | JP3692131B2 | 07 September 2005 (07-09-2005) |
| | | JP2001527659A | 25 December 2001 (25-12-2001) |
| | | JP4065963B2 | 26 March 2008 (26-03-2008) |
| | | JP2001515382A | 18 September 2001 (18-09-2001) |
| | | JP2002214127A | 31 July 2002 (31-07-2002) |
| | | US5321501A | 14 June 1994 (14-06-1994) |
| | | US5459570A | 17 October 1995 (17-10-1995) |
| | | US5465147A | 07 November 1995 (07-11-1995) |
| | | US5748598A | 05 May 1998 (05-05-1998) |
| | | US5784352A | 21 July 1998 (21-07-1998) |
| | | US5956355A | 21 September 1999 (21-09-1999) |
| | | US6111645A | 29 August 2000 (29-08-2000) |
| | | US6160826A | 12 December 2000 (12-12-2000) |
| | | US6282011B1 | 28 August 2001 (28-08-2001) |
| | | US2001036002A1 | 01 November 2001 (01-11-2001) |
| | | US6421164B2 | 16 July 2002 (16-07-2002) |
| | | US6485413B1 | 26 November 2002 (26-11-2002) |
| | | US6501551B1 | 31 December 2002 (31-12-2002) |
| | | US6564087B1 | 13 May 2003 (13-05-2003) |
| | | WO0042906A2 | 27 July 2000 (27-07-2000) |
| | | WO0042906A3 | 11 January 2001 (11-01-2001) |
| | | WO0042906B1 | 01 March 2001 (01-03-2001) |
| | | WO9219930A1 | 12 November 1992 (12-11-1992) |
| | | WO9533970A1 | 14 December 1995 (14-12-1995) |
| | | WO9533971A1 | 14 December 1995 (14-12-1995) |
| | | WO9701167A1 | 09 January 1997 (09-01-1997) |
| | | WO9723870A1 | 03 July 1997 (03-07-1997) |
| | | WO9732182A1 | 04 September 1997 (04-09-1997) |
| | | WO9835203A2 | 13 August 1998 (13-08-1998) |
| | | WO9835203A3 | 29 October 1998 (29-10-1998) |
| | | WO9838907A1 | 11 September 1998 (11-09-1998) |
| | | WO9852021A1 | 19 November 1998 (19-11-1998) |
| US6485413B1 | 26 November 2002 (26-11-2002) | AU1977597A | 16 September 1997 (16-09-1997) |
| | | CA2289598A1 | 19 November 1998 (19-11-1998) |
| | | CA2289598C | 20 July 2004 (20-07-2004) |
| | | DE69227902D1 | 28 January 1999 (28-01-1999) |
| | | DE69227902T2 | 17 June 1999 (17-06-1999) |

Continued in Supplemental Box

Patent family members continued

| | | | |
|---|---|---|---|
| | | DE69227902T3 | 22 April 2010 (22-04-2010) |
| | | DE69738291D1 | 27 December 2007 (27-12-2007) |
| | | DE69738291T2 | 11 September 2008 (11-09-2008) |
| | | DE69821610D1 | 18 March 2004 (18-03-2004) |
| | | DE69821610T2 | 23 December 2004 (23-12-2004) |
| | | EP0581871A1 | 09 February 1994 (09-02-1994) |
| | | EP0581871A4 | 27 April 1994 (27-04-1994) |
| | | EP0581871B1 | 16 December 1998 (16-12-1998) |
| | | EP0581871B2 | 12 August 2009 (12-08-2009) |
| | | EP0883793A1 | 16 December 1998 (16-12-1998) |
| | | EP0883793B1 | 14 November 2007 (14-11-2007) |
| | | EP0971626A1 | 19 January 2000 (19-01-2000) |
| | | EP0981733A1 | 01 March 2000 (01-03-2000) |
| | | EP0981733B1 | 11 February 2004 (11-02-2004) |
| | | JPH06511312A | 15 December 1994 (15-12-1994) |
| | | JP3479069B2 | 15 December 2003 (15-12-2003) |
| | | JP2000503237A | 21 March 2000 (21-03-2000) |
| | | JP3628026B2 | 09 March 2005 (09-03-2005) |
| | | JP2004105708A | 08 April 2004 (08-04-2004) |
| | | JP3692131B2 | 07 September 2005 (07-09-2005) |
| | | JP2001527659A | 25 December 2001 (25-12-2001) |
| | | JP4065963B2 | 26 March 2008 (26-03-2008) |
| | | JP2001515382A | 18 September 2001 (18-09-2001) |
| | | JP2002214127A | 31 July 2002 (31-07-2002) |
| | | US5321501A | 14 June 1994 (14-06-1994) |
| | | US5459570A | 17 October 1995 (17-10-1995) |
| | | US5465147A | 07 November 1995 (07-11-1995) |
| | | US5748598A | 05 May 1998 (05-05-1998) |
| | | US5784352A | 21 July 1998 (21-07-1998) |
| | | US5956355A | 21 September 1999 (21-09-1999) |
| | | US6111645A | 29 August 2000 (29-08-2000) |
| | | US6134003A | 17 October 2000 (17-10-2000) |
| | | US6160826A | 12 December 2000 (12-12-2000) |
| | | US6282011B1 | 28 August 2001 (28-08-2001) |
| | | US2001036002A1 | 01 November 2001 (01-11-2001) |
| | | US6421164B2 | 16 July 2002 (16-07-2002) |
| | | US6501551B1 | 31 December 2002 (31-12-2002) |
| | | US6564087B1 | 13 May 2003 (13-05-2003) |
| | | WO0042906A2 | 27 July 2000 (27-07-2000) |
| | | WO0042906A3 | 11 January 2001 (11-01-2001) |
| | | WO0042906B1 | 01 March 2001 (01-03-2001) |
| | | WO9219930A1 | 12 November 1992 (12-11-1992) |
| | | WO9533970A1 | 14 December 1995 (14-12-1995) |
| | | WO9533971A1 | 14 December 1995 (14-12-1995) |
| | | WO9701167A1 | 09 January 1997 (09-01-1997) |
| | | WO9723870A1 | 03 July 1997 (03-07-1997) |
| | | WO9732182A1 | 04 September 1997 (04-09-1997) |
| | | WO9835203A2 | 13 August 1998 (13-08-1998) |
| | | WO9835203A3 | 29 October 1998 (29-10-1998) |
| | | WO9838907A1 | 11 September 1998 (11-09-1998) |
| | | WO9852021A1 | 19 November 1998 (19-11-1998) |
| US2010280392A1 | 04 November 2010 (04-11-2010) | EP2194874A1 | 16 June 2010 (16-06-2010) |
| | | WO2009036561A1 | 26 March 2009 (26-03-2009) |
| US2001047137A1 | 29 November 2001 (29-11-2001) | AU6417599A | 26 April 2000 (26-04-2000) |
| | | US6816743B2 | 09 November 2004 (09-11-2004) |
| | | WO0019889A1 | 13 April 2000 (13-04-2000) |
| | | WO0019889A9 | 31 August 2000 (31-08-2000) |

| | | | |
|---|---|---|---|
| 专利名称(译) | 用于光学评估原位接近下牙槽神经的方法和系统 | | |
| 公开(公告)号 | EP2699165A1 | 公开(公告)日 | 2014-02-26 |
| 申请号 | EP2012774529 | 申请日 | 2012-01-04 |
| [标]申请(专利权)人(译) | 该ghaderi哈桑博士 | | |
| 申请(专利权)人(译) | 原因之一，HASSAN GHADERI博士 | | |
| 当前申请(专利权)人(译) | 原因之一，HASSAN GHADERI博士 | | |
| [标]发明人 | MOGHADDAM HASSAN GHADERI<br>GALLANT PASCAL<br>MERMUT OZZY<br>VEILLEUX ISRAEL | | |
| 发明人 | MOGHADDAM, HASSAN, GHADERI<br>GALLANT, PASCAL<br>MERMUT, OZZY<br>VEILLEUX, ISRAËL | | |
| IPC分类号 | A61B6/14 A61C8/00 A61B5/026 A61B5/00 A61B5/1455 A61B17/16 A61B17/17 A61C1/08 A61C19/04 | | |
| CPC分类号 | A61B17/1703 A61B5/0066 A61B5/0075 A61B5/0261 A61B5/14551 A61B5/4542 A61B5/489 A61B5/4893 A61B17/1673 A61B2034/2057 A61B2090/306 A61C1/084 A61C1/088 A61C8/0089 A61C19/04 | | |
| 优先权 | 61/477787 2011-04-21 US<br>13/329557 2011-12-19 US | | |
| 其他公开文献 | EP2699165A4<br>EP2699165B1 | | |
| 外部链接 | Espacenet | | |


摘要(译)

用于评估与组织层的接近度的低相干干涉测量探针系统，包括用于产生低相干激发光的低相干光源，用于在组织层附近带来低相干激发光的激发光纤和用于捕获的回收光纤来自组织层的散射光。探针系统包括低相干干涉测量子系统和数字信号处理器，用于基于由采集光纤接收的背散射光来评估到组织层的距离。还提供了一种用于评估动脉接近度的光谱吸收探针系统，包括用于产生具有适于血液生色团吸收的波长的激发光的光源，用于在动脉附近产生激发光的激发光纤和收集光学系统。用于捕获动脉背散射光的光纤。该探针系统包括光检测器和信号处理器，用于基于背散射光确定到动脉的距离，并且使用围绕组织衰减系数（μe10）的值的Beer-Lambert光吸收定律。还提供了结合低相干干涉测量和光谱吸收的光谱吸收和低相干干涉测量探针系统。